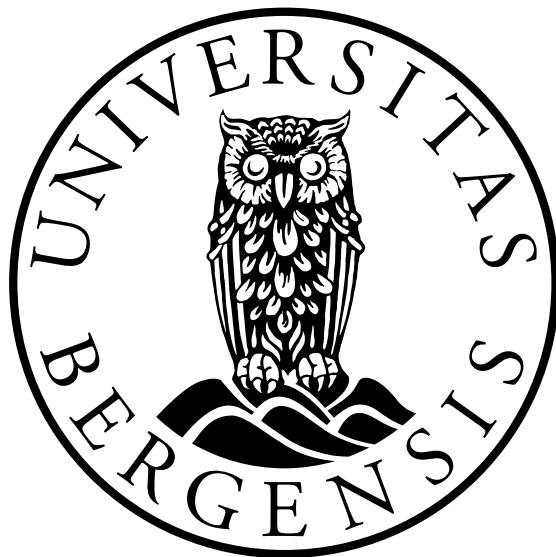


Title goes here

Author



Dissertation for the degree of Philosophiae Doctor (PhD)

Department of Physics and Technology
University of Bergen

Month year

Scientific environment

This is where you write the name of the subject/professional milieu involved in the study, faculty(faculties)/institute(s)/centre(s)/research groups/school of research.

Contractual joint venture partners should also be mentioned here. If these are represented by graphic symbols (logo etc.) the it should be on this page.

NB! Most organisations have guidelines concerning the use of their logo. These guidelines regulate who can use the logo, when the logo can be used and how. This is quite relevant when a logo is used together with information connected to other institutions/organisations. (A typical example would be rules concerning space between other written or graphic content.)

Remember to find out which guidelines apply and ensure that they are followed! Most organisations will be able to provide a digital version of their logo in a suitable format.

Acknowledgements

I would like to thank...

Abstract

This is where you write the abstract, ref:

”§ 6.6 Abstract of dissertation, press release

An abstract of the dissertation shall be prepared in English (1-3 pages), so that research environments in Norway and abroad may familiarize themselves with the results. The abstract shall accompany the dissertation.”

From ”The Regulations for the degree philosophiae doctor (PhD) at the University of Bergen”

(There is an abstract template that has room for information about the debate, opponent etc that can be used as a handout.)

List of papers

1. Author, *Sometitle*, Somejournal **1**, 1, 1905.

Contents

Scientific environment	i
Acknowledgements	iii
Abstract	v
List of papers	vii
1 Introduction	1
2 Introduction to the papers	3
3 Scientific results	5
3.1 Paper title	7
3.2 Paper title	19
3.3 Paper title	39
A Some appendix	61

List of Figures

Listings

Chapter 1

Introduction

This is the introduction [1, 2]...

Chapter 2

Introduction to the papers

Paper I: *Title*

In this paper...

Chapter 3

Scientific results

Paper A

3.1 Paper title

List of authors

Physical Review B, **76**, 035303 (2007)



The Whitham Equation as a model for surface water waves



Daulet Moldabayev^a, Henrik Kalisch^{a,*}, Denys Dutykh^b

^a Department of Mathematics, University of Bergen, Postbox 7800, 5020 Bergen, Norway

^b LAMA, UMR5127, CNRS – Université Savoie Mont Blanc, 73376 Le Bourget-du-Lac Cedex, France

HIGHLIGHTS

- Definition of Whitham scaling regime.
- Derivation of a Hamiltonian Whitham system.
- Asymptotic derivation of the Whitham equation.
- Comparison of Whitham, KdV, BBM and Padé models with inviscid free surface dynamics.

ARTICLE INFO

Article history:

Received 16 October 2014

Received in revised form

9 June 2015

Accepted 24 July 2015

Available online 31 July 2015

Communicated by J. Bronski

Keywords:

Nonlocal equations
Nonlinear dispersive equations
Hamiltonian models
Solitary waves
Surface waves

ABSTRACT

The Whitham equation was proposed as an alternate model equation for the simplified description of unidirectional wave motion at the surface of an inviscid fluid. As the Whitham equation incorporates the full linear dispersion relation of the water wave problem, it is thought to provide a more faithful description of shorter waves of small amplitude than traditional long wave models such as the KdV equation.

In this work, we identify a scaling regime in which the Whitham equation can be derived from the Hamiltonian theory of surface water waves. A Hamiltonian system of Whitham type allowing for two-way wave propagation is also derived. The Whitham equation is integrated numerically, and it is shown that the equation gives a close approximation of inviscid free surface dynamics as described by the Euler equations. The performance of the Whitham equation as a model for free surface dynamics is also compared to different free surface models: the KdV equation, the BBM equation, and the Padé (2,2) model. It is found that in a wide parameter range of amplitudes and wavelengths, the Whitham equation performs on par with or better than the three considered models.

© 2015 The Authors. Published by Elsevier B.V.
This is an open access article under the CC BY-NC-ND license
(<http://creativecommons.org/licenses/by-nc-nd/4.0/>).

1. Introduction

In its simplest form, the water-wave problem concerns the flow of an incompressible inviscid fluid with a free surface over a horizontal impenetrable bed. In this situation, the fluid flow is described by the Euler equations with appropriate boundary conditions, and the dynamics of the free surface are of particular interest in the solution of this problem.

There are a number of model equations which allow the approximate description of the evolution of the free surface without having to provide a complete solution of the fluid flow below the surface. In the present contribution, interest is focused

on the derivation and evaluation of a nonlocal water-wave model known as the Whitham equation. The equation is written as

$$\eta_t + \frac{3}{2} \frac{c_0}{h_0} \eta \eta_x + K_{h_0} * \eta_x = 0, \quad (1)$$

where the convolution kernel K_{h_0} is given in terms of the Fourier transform by

$$\mathcal{F}K_{h_0}(\xi) = \sqrt{\frac{g \tanh(h_0 \xi)}{\xi}}, \quad (2)$$

g is the gravitational acceleration, h_0 is the undisturbed depth of the fluid, and $c_0 = \sqrt{gh_0}$ is the corresponding long-wave speed. The convolution can be thought of as a Fourier multiplier operator, and (2) represents the Fourier symbol of the operator.

The Whitham equation was proposed by Whitham [1] as an alternative to the well known Korteweg-de Vries (KdV) equation

$$\eta_t + c_0 \eta_x + \frac{3}{2} \frac{c_0}{h_0} \eta \eta_x + \frac{1}{6} c_0 h_0^2 \eta_{xxx} = 0. \quad (3)$$

* Corresponding author.

E-mail addresses: daulet.moldabayev@math.uib.no (D. Moldabayev), henrik.kalisch@math.uib.no (H. Kalisch), Denys.Dutykh@univ-savoie.fr (D. Dutykh).

<http://dx.doi.org/10.1016/j.physd.2015.07.010>

0167-2789/© 2015 The Authors. Published by Elsevier B.V. This is an open access article under the CC BY-NC-ND license (<http://creativecommons.org/licenses/by-nc-nd/4.0/>).

The validity of the KdV equation as a model for surface water waves can be described as follows. Suppose a wave field with a prominent amplitude a and characteristic wavelength l is to be studied. The KdV equation is known to produce a good approximation of the evolution of the waves if the amplitude of the waves is small and the wavelength is large when compared to the undisturbed depth, and if in addition, the two non-dimensional quantities a/h_0 and h_0^2/l^2 are of similar size. The latter requirement can be written in terms of the Stokes number as

$$\delta = \frac{al^2}{h_0^3} \sim 1.$$

While the KdV equation is a good model for surface waves if $\delta \sim 1$, one notorious problem with the KdV equation is that it does not model accurately the dynamics of shorter waves. Recognizing this shortcoming of the KdV equation, Whitham proposed to use the same nonlinearity as the KdV equation, but couple it with a linear term which mimics the linear dispersion relation of the full water-wave problem. Thus, at least in theory, the Whitham equation can be expected to yield a description of the dynamics of shorter waves which is closer to the solutions of the more fundamental Euler equations which govern the flow.

The Whitham equation has been studied from a number of vantage points during recent years. In particular, the existence of traveling and solitary waves has been established in [2,3]. Well posedness of a similar equation was investigated in [4–6], and a model with variable depth has been studied numerically in [7]. Moreover, it has been shown in [8,9] that periodic solutions of the Whitham equation feature modulational instability for short enough waves in a similar way as small-amplitude periodic wave solutions of the water-wave problem. However, even though the equation is routinely mentioned in texts on nonlinear waves [10, 11], it appears that the performance of the Whitham equation in the description of surface water waves has not been investigated so far.

The purpose of the present article is to give an asymptotic derivation of the Whitham equation as a model for surface water waves, and to confirm Whitham's expectation that the equation is a fair model for the description of time-dependent surface water waves. For the purpose of the derivation, we introduce an exponential scaling regime in which the Whitham equation can be derived asymptotically from an approximate Hamiltonian principle for surface water waves. In order to motivate the use of this scaling, note that the KdV equation has the property that wide classes of initial data decompose into a number of solitary waves and small-amplitude dispersive residue [12]. For the KdV equations, solitary-wave solutions are known in closed form, and are given by

$$\eta = \frac{a}{h_0} \operatorname{sech}^2 \left(\sqrt{\frac{3a}{4h_0^3}} (x - ct) \right) \quad (4)$$

for a certain wave celerity c . These waves clearly comply with the amplitude-wavelength relation $a/h_0 \sim h_0^2/l^2$ which was mentioned above. It appears that the Whitham equation – as indeed do many other nonlinear dispersive equations – also has the property that broad classes of initial data rapidly decompose into ordered trains of solitary waves (see Fig. 1). Quantifying the amplitude-wavelength relation for these solitary waves yields an asymptotic regime which is expected to be relevant to the validity of the Whitham equation as a water wave model.

As the curve fit in the right panel of Fig. 1 shows, the relationship between wavelength and amplitude of the Whitham solitary waves can be approximately described by the relation $\frac{a}{h_0} \sim e^{-\kappa(l/h_0)^v}$ for certain values of κ and v . Since the Whitham solitary waves are not known in exact form, the values of κ and v have to be found numerically. Then one may define a Whitham scaling regime

$$\mathcal{W}(\kappa, v) = \frac{a}{h_0} e^{\kappa(l/h_0)^v} \sim 1, \quad (5)$$

and it will be shown in Sections 2 and 3 that this scaling can be used advantageously in the derivation of the Whitham equation. The derivation proceeds by examining the Hamiltonian formulation of the water-wave problem due to Zakharov, Craig and Sulem [13,14], and by restricting to wave motion which is predominantly in the direction of increasing values of x . The approach is similar to the method of [15], but relies on the new relation (5).

First, in Section 2, a Whitham system is derived which allows for two-way propagation of waves. The Whitham equation is found in Section 3. Finally, in Section 4, a comparison of modeling properties of the KdV and Whitham equations is given. The comparison also includes the regularized long-wave equation

$$\eta_t + c_0 \eta_x + \frac{3}{2} \frac{c_0}{h_0} \eta \eta_x - \frac{1}{6} h_0^2 \eta_{xxt} = 0, \quad (6)$$

which was put forward in [16] and studied in depth in [17], and which is also known as the BBM or PBBM equation. The linearized dispersion relation of this equation is not an exact match to the dispersion relation of the full water-wave problem, but it is much closer than the KdV equation, and it might also be expected that this equation may be able to model shorter waves more successfully than the KdV equation. In order to obtain an even better match of the linear dispersion relation, one may make use of Padé expansions. In the context of simplified evolutions equations, this approach was pioneered in [18]. For uni-directional models, this approach was advocated in [19], and in particular, the equation based on the Padé (2,2) approximation was studied in depth. In dimensional variables, this model takes the form

$$\eta_t + c_0 \eta_x + \frac{3}{2} \frac{c_0}{h_0} \eta \eta_x - \frac{3}{20} c_0 h_0^2 \eta_{xxx} - \frac{19}{60} h_0^2 \eta_{xxt} = 0. \quad (7)$$

The dispersion relations for the KdV, BBM and Padé (2,2) models are respectively

$$\begin{aligned} c(k) &= c_0 - \frac{1}{6} c_0 h_0^2 k^2 && (\text{KdV}), \\ c(k) &= \frac{1}{1 + \frac{1}{6} h_0^2 k^2} && (\text{BBM}), \\ c(k) &= c_0 \frac{1 + \frac{3}{20} h_0^2 k^2}{1 + \frac{19}{60} h_0^2 k^2} && (\text{Padé (2,2)}). \end{aligned}$$

These approximate dispersion relations are compared to the full dispersion relation in Fig. 2. It appears clearly that the Padé (2,2) approximation remains much closer to the full dispersion relation than the dispersion relations based on either the linear KdV or linear BBM equations. As will be seen in Section 4, solutions of both the Whitham and Padé (2,2) equations give closer approximations to solutions of the full Euler equations than either the KdV or BBM equations in most cases investigated. However, the Whitham equation still keeps a slight edge over the Padé model.

2. Derivation of evolution systems of Whitham type

The surface water-wave problem is generally described by the Euler equations with slip conditions at the bottom, and kinematic and dynamic boundary conditions at the free surface. Assuming weak transverse effects, the unknowns are the surface elevation $\eta(x, t)$, the horizontal and vertical fluid velocities $u_1(x, z, t)$ and $u_2(x, z, t)$, respectively, and the pressure $P(x, z, t)$. If the assumption of irrotational flow is made, then a velocity potential $\phi(x, z, t)$ can be used. In order to nondimensionalize the problem, the undisturbed depth h_0 is taken as a unit of distance, and the

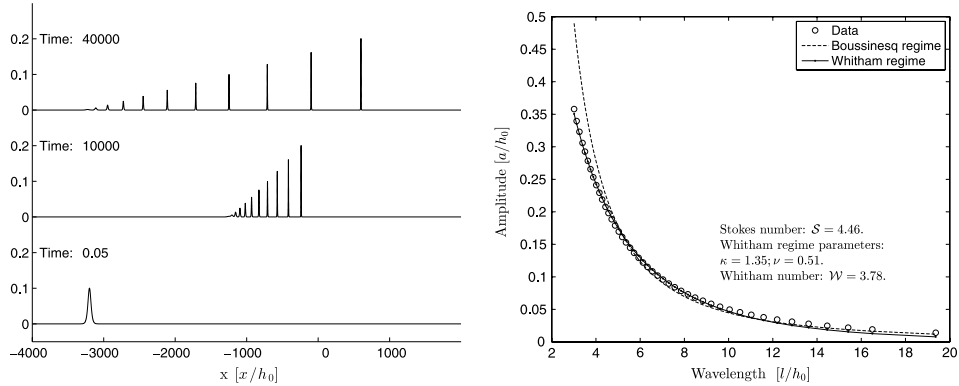


Fig. 1. Left panel: Formation of solitary waves of the Whitham equation from Gaussian initial data. Right panel: Curve fit for the Whitham regime and for the Boussinesq regime to amplitude/wavelength data from Whitham solitary waves. The wavelength is defined as $l = \frac{1}{a} \int_{-\infty}^{\infty} \eta(x) dx$.

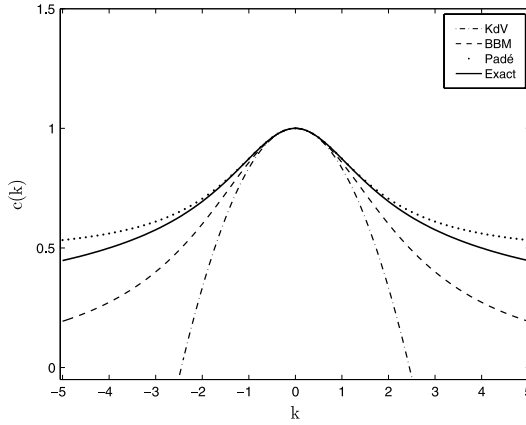


Fig. 2. Approximate models to the exact dispersion relation of the full water-wave problem.

parameter $\sqrt{h_0/g}$ as a unit of time. For the remainder of this article, all variables appearing in the water-wave problem are considered as being non-dimensional. The problem is posed on a domain $\{(x, z)^T \in \mathbb{R}^2 \mid -1 < z < \eta(x, t)\}$ which extends to infinity in the positive and negative x -direction. Due to the incompressibility of the fluid, the potential then satisfies Laplace's equation in this domain. The fact that the fluid cannot penetrate the bottom is expressed by a homogeneous Neumann boundary condition at the flat bottom. Thus we have

$$\begin{aligned} \phi_{xx} + \phi_{zz} &= 0 \quad \text{in } -1 < z < \eta(x, t) \\ \phi_z &= 0 \quad \text{on } z = -1. \end{aligned}$$

The pressure is eliminated with the help of the Bernoulli equation, and the free-surface boundary conditions are formulated in terms of the potential and the surface excursion by

$$\left. \begin{aligned} \eta_t + \phi_x \eta_x - \phi_z &= 0, \\ \phi_t + \frac{1}{2} (\phi_x^2 + \phi_z^2) + \eta &= 0, \end{aligned} \right\} \text{on } z = \eta(x, t).$$

The total energy of the system is given by the sum of kinetic energy and potential energy, and normalized such that the potential energy is zero when no wave motion is present at the surface. Accordingly the Hamiltonian function for this problem is

$$H = \int_{\mathbb{R}} \int_0^{\eta} z dz dx + \int_{\mathbb{R}} \int_{-1}^{\eta} \frac{1}{2} |\nabla \phi|^2 dz dx. \quad (8)$$

Defining the trace of the potential at the free surface as $\Phi(x, t) = \phi(x, \eta(x, t), t)$, one may integrate in z in the first integral and use the divergence theorem on the second integral in order to arrive at the formulation

$$H = \frac{1}{2} \int_{\mathbb{R}} [\eta^2 + \Phi G(\eta) \Phi] dx. \quad (9)$$

This is the Hamiltonian formulation of the water wave problem as found in [13,20,14], and written in terms of the Dirichlet–Neumann operator $G(\eta)$. As shown in [21], the Dirichlet–Neumann operator can be expanded in a series of the form

$$G(\eta) \Phi = \sum_{j=0}^{\infty} G_j(\eta) \Phi. \quad (10)$$

In order to proceed, we need to understand the first few terms in this series. As shown in [15,13], the first two terms in this series can be written with the help of the operator $D = -i\partial_x$ as

$$G_0(\eta) = D \tanh(D), \quad G_1(\eta) = D\eta D - D \tanh(D) \eta D \tanh(D).$$

Note that it can be shown that the terms $G_j(\eta)$ for $j \geq 2$ are of quadratic or higher-order in η , and will therefore not be needed in the current analysis.

It will be convenient for the present purpose to formulate the Hamiltonian in terms of the dependent variable $u = \Phi_x$. To this end, we define the operator $\mathcal{K}(\eta)$ by

$$G(\eta) = D \mathcal{K}(\eta) D.$$

As was the case with $G(\eta)$, the operator $\mathcal{K}(\eta)$ can be expanded in a Taylor series around zero as

$$\mathcal{K}(\eta) \xi = \sum_{j=0}^{\infty} \mathcal{K}_j(\eta) \xi, \quad \mathcal{K}_j(\eta) = D^{-1} G_j(\eta) D^{-1}. \quad (11)$$

In particular, note that $\mathcal{K}_0 = \frac{\tanh D}{D}$. In non-dimensional variables, we write the operator with the integral kernel K_{h_0} as $K = \sqrt{\frac{\tanh D}{D}}$, so that we have $\mathcal{K}_0 = K^2$. The Hamiltonian is then expressed as

$$H = \frac{1}{2} \int_{\mathbb{R}} [\eta^2 + u \mathcal{K}(\eta) u] dx. \quad (12)$$

The water-wave problem can then be written as a Hamiltonian system using the variational derivatives of H and posing the Hamiltonian equations

$$\eta_t = -\partial_x \frac{\delta H}{\delta u}, \quad u_t = -\partial_x \frac{\delta H}{\delta \eta}. \quad (13)$$

This system is not in canonical form as the associated structure map $J_{\eta,u}$ is symmetric:

$$J_{\eta,u} = \begin{pmatrix} 0 & -\partial_x \\ -\partial_x & 0 \end{pmatrix}.$$

We now proceed to derive a system of equations which is similar to the Whitham equation (1), but allows bi-directional wave propagation. This system will be a stepping stone on the way to a derivation of (1), but may also be of independent interest. Consider a wave-field having a characteristic wavelength l and a characteristic amplitude a . Taking into account the nondimensionalization, the two scalar parameters $\lambda = l/h_0$ and $\alpha = a/h_0$ appear. In order to introduce the long-wave and small amplitude approximation into the non-dimensional problem, we use the scaling $\tilde{x} = \frac{1}{\lambda}x$, and $\eta = \alpha\tilde{\eta}$. This induces the transformation $\tilde{D} = \lambda D = -\lambda i\partial_x$. If the energy is nondimensionalized in accord with the nondimensionalization mentioned earlier, then the natural scaling for the Hamiltonian is $\tilde{H} = \alpha^2 H$. In addition, the unknown u is scaled as $u = \alpha\tilde{u}$. The scaled Hamiltonian (12) is then written as

$$\begin{aligned} \tilde{H} = & \frac{1}{2} \int_{\mathbb{R}} \tilde{\eta}^2 dx + \frac{1}{2} \int_{\mathbb{R}} \tilde{u} \left[1 - \frac{1}{3} \lambda^{-2} \tilde{D}^2 + \dots \right] \tilde{u} dx \\ & + \frac{\alpha}{2} \int_{\mathbb{R}} \tilde{\eta} \tilde{u}^2 dx - \frac{\alpha}{2} \int_{\mathbb{R}} \tilde{u} \left[\lambda^{-1} \tilde{D} - \frac{1}{3} \lambda^{-3} \tilde{D}^3 + \dots \right] \\ & \times \tilde{\eta} \left[\lambda^{-1} \tilde{D} - \frac{1}{3} \lambda^{-3} \tilde{D}^3 + \dots \right] \tilde{u} dx. \end{aligned}$$

Let us now introduce the small parameter $\mu = \frac{1}{\lambda}$, and assume for simplicity that $\alpha = e^{-\kappa/\mu^v}$, which corresponds to the case where $\mathcal{W}(\kappa, v) = 1$. Then the Hamiltonian can be written in the following form:

$$\begin{aligned} \tilde{H} = & \frac{1}{2} \int_{\mathbb{R}} \tilde{\eta}^2 dx + \frac{1}{2} \int_{\mathbb{R}} \tilde{u} \left[1 - \frac{1}{3} \mu^2 \tilde{D}^2 + \dots \right] \tilde{u} dx \\ & + \frac{e^{-\kappa/\mu^v}}{2} \int_{\mathbb{R}} \tilde{\eta} \tilde{u}^2 dx - \frac{e^{-\kappa/\mu^v}}{2} \int_{\mathbb{R}} \tilde{u} \left[\mu \tilde{D} - \frac{1}{3} \mu^3 \tilde{D}^3 + \dots \right] \\ & \times \tilde{\eta} \left[\mu \tilde{D} - \frac{1}{3} \mu^3 \tilde{D}^3 + \dots \right] \tilde{u} dx. \end{aligned}$$

Disregarding terms of order $\mathcal{O}(\mu^2 e^{-\kappa/\mu^v})$, but not of order $\mathcal{O}(e^{-\kappa/\mu^v})$ yields the expansion

$$\begin{aligned} \tilde{H} = & \frac{1}{2} \int_{\mathbb{R}} \tilde{\eta}^2 dx + \frac{1}{2} \int_{\mathbb{R}} \tilde{u} \left[1 - \frac{1}{3} \mu^2 \tilde{D}^2 + \dots \right] \tilde{u} dx \\ & + \frac{e^{-\kappa/\mu^v}}{2} \int_{\mathbb{R}} \tilde{\eta} \tilde{u}^2 dx. \end{aligned} \quad (14)$$

Note that by taking μ small enough, an arbitrary number of terms of algebraic order in μ may be kept in the asymptotic series, so that the truncated version of the Hamiltonian in dimensional variables may be written as

$$H = \frac{1}{2} \int_{\mathbb{R}} [\eta^2 + u \mathcal{K}_0^N(\eta)u + u\eta u] dx dz. \quad (15)$$

However, the difference between \mathcal{K}_0 and \mathcal{K}_0^N is below the order of approximation, so that it is possible to formally define the truncated Hamiltonian with \mathcal{K}_0 instead of \mathcal{K}_0^N .

Hence, the Whitham system is obtained from the Hamiltonian (15) as follows:

$$\eta_t = -\partial_x \frac{\delta H}{\delta u} = -\mathcal{K}_0 u_x - (\eta u)_x, \quad (16)$$

$$u_t = -\partial_x \frac{\delta H}{\delta \eta} = -\eta_x - uu_x. \quad (17)$$

One may also derive a higher-order equation by keeping terms of order $\mathcal{O}(\mu^2 e^{-\kappa/\mu^v})$, but discarding terms of order $\mathcal{O}(\mu^4 e^{-\kappa/\mu^v})$. In this case we find the system

$$\eta_t = -\mathcal{K}_0 u_x - (\eta u)_x - (\eta u_x)_{xx},$$

$$u_t = -\eta_x - uu_x + u_x u_{xx}.$$

3. Derivation of evolution equations of Whitham type

In order to derive the Whitham equation for uni-directional wave propagation, it is important to understand how solutions of the Whitham system (16)–(17) can be restricted to either left or right-going waves. As it will turn out, if η and u are such that $\eta = Ku$, then this pair of functions represents a solution of (16)–(17) which is propagating to the right. Indeed, let us analyze the relation between η and u in the linearized Whitham system

$$\eta_t = -\mathcal{K}_0 u_x, \quad (18)$$

$$u_t = -\eta_x. \quad (19)$$

Considering a solution of the system (18)–(19) in the form

$$\eta(x, t) = Ae^{(i\xi x - i\omega t)}, \quad u(x, t) = Be^{(i\xi x - i\omega t)}, \quad (20)$$

gives rise to the matrix equation

$$\begin{pmatrix} -\omega & \tanh \xi \\ \xi & -\omega \end{pmatrix} \begin{pmatrix} A \\ B \end{pmatrix} = \begin{pmatrix} 0 \\ 0 \end{pmatrix}. \quad (21)$$

If existence of a nontrivial solution of this system is to be guaranteed, the determinant of the matrix has to be zero, so that we have $\omega^2 - \frac{\tanh \xi}{\xi} \xi^2 = 0$. Defining the phase speed as $c = \omega/\xi$, we obtain the dispersion relation

$$c = \pm \sqrt{\frac{\tanh \xi}{\xi}}. \quad (22)$$

The choice of $c > 0$ corresponds to right-going wave solutions of the system (18)–(19), and the relation between η and u can be deduced from (19). Accordingly, it is expedient to separate solutions into a right-going part r and a left-going part s which are defined by

$$r = \frac{1}{2}(\eta + Ku), \quad s = \frac{1}{2}(\eta - Ku).$$

According to the transformation theory detailed in [22], if the unknowns r and s are used instead of η and u , the structure map changes to

$$J_{r,s} = \left(\frac{\partial F}{\partial(r, u)} \right) J_{\eta,u} \left(\frac{\partial F}{\partial(\eta, u)} \right)^T = \begin{pmatrix} -\frac{1}{2} \partial_x K & 0 \\ 0 & \frac{1}{2} \partial_x K \end{pmatrix}. \quad (23)$$

We now use the same scaling for both dependent and independent variables as before. Thus we have $r = \alpha\tilde{r}$ and $s = \alpha\tilde{s}$. The Hamiltonian is written in terms of \tilde{r} and \tilde{s} as

$$\begin{aligned} \tilde{H} = & \frac{1}{2} \int_{\mathbb{R}} (\tilde{r} + \tilde{s})^2 dx \\ & + \frac{1}{2} \int_{\mathbb{R}} \tilde{K}^{-1}(\tilde{r} - \tilde{s}) \left[1 - \frac{1}{3} \mu^2 \tilde{D}^2 + \dots \right] \tilde{K}^{-1}(\tilde{r} - \tilde{s}) dx \\ & + \frac{\alpha}{2} \int_{\mathbb{R}} (\tilde{r} + \tilde{s}) \left(\tilde{K}^{-1}(\tilde{r} - \tilde{s}) \right)^2 dx \\ & - \frac{\alpha}{2} \int_{\mathbb{R}} \tilde{K}^{-1}(\tilde{r} - \tilde{s}) \left[\mu \tilde{D} - \frac{1}{3} \mu^3 \tilde{D}^3 + \dots \right] (\tilde{r} + \tilde{s}) \\ & \times \left[\mu \tilde{D} - \frac{1}{3} \mu^3 \tilde{D}^3 + \dots \right] \tilde{K}^{-1}(\tilde{r} - \tilde{s}) dx. \end{aligned}$$

Following the transformation rules, the structure map transforms to $J_{\tilde{r},\tilde{s}} = 1/\alpha^2 J_{r,s}$. In addition, the time scaling $t = \lambda \tilde{t}$ is employed. Since the focus is on right-going solutions, the equation to be considered is

$$\lambda \tilde{r}_{\tilde{t}} = -\frac{1}{2\alpha^2} \lambda \partial_{\tilde{x}} \tilde{K} \left[\frac{\delta(\alpha^2 \tilde{H})}{\delta \tilde{r}} \right]. \quad (24)$$

So far, this equation is exact. If we now assume that s is of the order of $\mathcal{O}(\mu^2 e^{-\kappa/\mu^\nu})$, then the equation for \tilde{r} is

$$\begin{aligned} \tilde{r}_{\tilde{t}} = & -\frac{1}{2} \partial_{\tilde{x}} \left[1 - \frac{1}{6} \mu^2 \tilde{D}^2 + \dots \right] \left\{ 2\tilde{r} + \frac{\alpha}{2} \left([1 + \frac{1}{6} \mu^2 \tilde{D}^2 + \dots] \tilde{r} \right)^2 \right. \\ & + \alpha \left[1 + \frac{1}{6} \mu^2 \tilde{D}^2 + \dots \right] \left(\tilde{r} [1 + \frac{1}{6} \mu^2 \tilde{D}^2 + \dots] \tilde{r} \right) \\ & - \frac{\alpha}{2} \left([\mu \tilde{D} - \frac{1}{3} \mu^3 \tilde{D}^3 + \dots] [1 + \frac{1}{6} \mu^2 \tilde{D}^2 + \dots] \tilde{r} \right)^2 \\ & - \alpha \left[\mu \tilde{D} - \frac{1}{3} \mu^3 \tilde{D}^3 + \dots \right] \left[1 + \frac{1}{6} \mu^2 \tilde{D}^2 + \dots \right] \\ & \times \left(\tilde{r} [\mu \tilde{D} - \frac{1}{3} \mu^3 \tilde{D}^3 + \dots] [1 + \frac{1}{6} \mu^2 \tilde{D}^2 + \dots] \tilde{r} \right) \left. \right\} \\ & + \mathcal{O}(\alpha \mu^2). \end{aligned}$$

As in the case of the Whitham system, we use $\alpha = \mathcal{O}(e^{-\kappa/\mu^\nu})$, and disregard terms of order $\mathcal{O}(\mu^2 e^{-\kappa/\mu^\nu})$, but not of order $\mathcal{O}(e^{-\kappa/\mu^\nu})$. This procedure yields the Whitham equation (1) which is written in nondimensional variables as

$$r_t = -Kr_x - \frac{3}{2}rr_x.$$

As was the case for the system found in the previous section, it is also possible here to include terms of order $\mathcal{O}(\mu^2 e^{-\kappa/\mu^\nu})$, resulting in the higher-order equation

$$r_t = -Kr_x - \frac{3}{2}rr_x - \frac{13}{12}r_x r_{xx} - \frac{5}{12}rr_{xxx}.$$

4. Numerical results

In this section, the performance of the Whitham equation as a model for surface water waves is compared to the KdV equation (3), the BBM equation (6), and the Padé (2,2) equation (7). For this purpose initial data are imposed, the Whitham, KdV, BBM, and Padé equations are solved numerically, and the solutions are compared to numerical solutions of the full Euler equations with free-surface boundary conditions. We continue to work in normalized variables, such as stated in the beginning of Section 2.

The numerical treatment of the three model equations is by a standard pseudo-spectral scheme, such as explained in [23,24] for example. For the time stepping, an efficient fourth-order implicit method developed in [25] is used. The numerical treatment of the free-surface problem for the Euler equations is based on a conformal mapping of the fluid domain into a rectangle. In the time-dependent case, this method has roots in the work of Ovsyannikov [26], and was later used in [27–30]. The particular method used for the numerical experiments reported here is a pseudo-spectral scheme which is detailed in [31].

Initial conditions for the Euler equations are chosen in such a way that the solutions are expected to be right moving. This is achieved by posing an initial surface disturbance $\eta_0(x)$ together with the trace of the potential $\Phi(x) = \int_0^x \eta_0(x') dx'$. In order to normalize the data, we choose $\eta_0(x)$ in such a way that the average of $\eta_0(x)$ over the computational domain is zero. The experiments are performed with several different amplitudes α and wavelengths

Table 1

Summary of the Stokes number, nondimensional amplitude and nondimensional wavelength of the initial data used in the numerical experiments.

Experiment	Stokes number	α	λ
A	0.2	0.1	$\sqrt{2}$
B	0.2	0.2	1
C	1	0.1	$\sqrt{10}$
D	1	0.2	$\sqrt{5}$
E	5	0.1	$\sqrt{50}$
F	5	0.2	5

(for the purpose of this section, we define the wavelength λ as the distance between the two points x_1 and x_2 at which $\eta_0(x_1) = \eta_0(x_2) = \alpha/2$). Both positive and negative initial disturbances are considered. While disturbances with positive main part have been studied widely, an initial wave of depression is somewhat more exotic, but nevertheless important, as shown for instance in [32]. A summary of the experiments' settings is given in Table 1. Experiments run with an initial wave of elevation are labeled as *positive*, and experiments run with an initial wave of depression are labeled as *negative*. The domain for the computations is $-L \leq x \leq L$, with $L = 50$. The function initial data in the *positive* cases is given by

$$\eta_0(x) = \alpha \operatorname{sech}^2(f(\lambda)x) - C, \quad (25)$$

where

$$f(\lambda) = \frac{2}{\lambda} \log \left(\frac{1 + \sqrt{1/2}}{\sqrt{1/2}} \right), \quad \text{and} \quad C = \frac{1}{L} \frac{\alpha}{f(\lambda)} \tanh \left(\frac{L}{f(\lambda)} \right)$$

and C and $f(\lambda)$ are chosen so that $\int_{-L}^L \eta_0(x) dx = 0$, and the wavelength λ is the distance between the two points x_1 and x_2 at which $\eta_0(x_1) = \eta_0(x_2) = \alpha/2$. The velocity potential in this case is given by

$$\Phi(x) = \frac{\alpha}{f(\lambda)} \tanh(f(\lambda)x) - Cx. \quad (26)$$

In the *negative* case, the initial data are given by

$$\eta_0(x) = -\alpha \operatorname{sech}^2(f(\lambda)x) + C.$$

The definitions for $f(\lambda)$ and C are the same, and the velocity potential is

$$\Phi(x) = -\frac{\alpha}{f(\lambda)} \tanh(f(\lambda)x) + Cx.$$

In Figs. 3 and 4, the time evolution of a wave with an initial narrow peak and one with an initial narrow depression at the center is shown. The amplitude is $\alpha = 0.2$, and the wavelength is $\lambda = \sqrt{5}$. In Fig. 3, the time evolution according to the Euler, Whitham, KdV and BBM equations are shown, and in Fig. 4, the time evolution according to the Euler, Whitham, and Padé (2,2) equations are shown.

It appears in Fig. 3 that the KdV equation produces a significant number of spurious oscillations, the BBM equation also produces a fair number of spurious oscillations, and the Whitham equation produces fewer small oscillations than Euler equations. Moreover, while the highest peak in the upper panels in Fig. 3 is underpredicted by the KdV and BBM equation, the Whitham equation produces peaks which are slightly too high. In the case of an initial depression, the Whitham equation also produces some peaks which are too high, but on the other hand, the KdV and the BBM equations introduce phase errors in the main oscillations. As is visible in Fig. 4, the Padé (2,2) equation reproduces the leading wave fairly accurately, but overpredicts the trailing oscillations in the case of a positive disturbance, and underpredicts the trailing oscillations in the case of a negative initial disturbance. Nevertheless, since the Padé (2,2) does not introduce a phase error, the overall performance is better than that of the KdV and BBM equations.

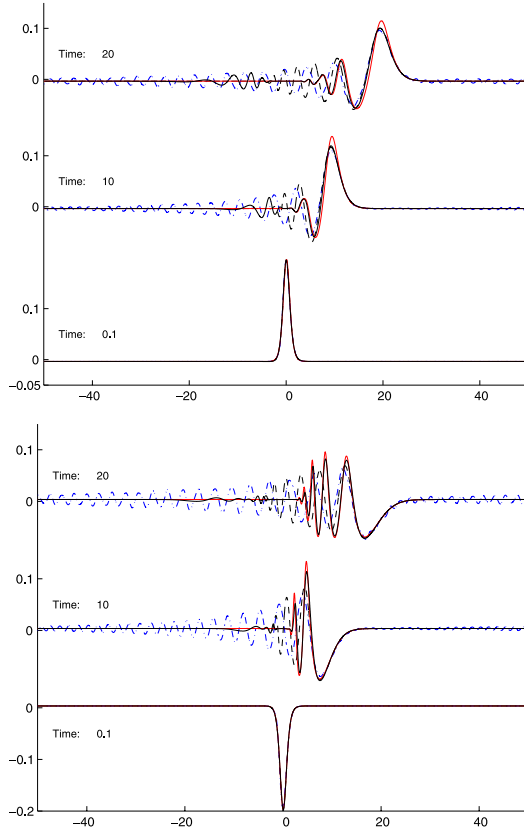


Fig. 3. Wave profiles at three different times: – Euler (black line), --- KdV, -·- BBM, – Whitham (red line). Experiment D: $\delta = 1$, $\alpha = 0.2$, $\lambda = \sqrt{5}$. Upper panel: positive case; lower panel: negative case. Horizontal axis: x/h_0 , vertical axis: z/h_0 . Snapshots are given at nondimensional time $t/\sqrt{h_0/g}$.

In order to compare the performance of the four approximate equations in a more quantitative manner, the discrepancies between solutions of the model equations and the prediction due to solving the Euler equations are measured in an integral norm. In the center right panels of Figs. 5 and 6, the computations from Figs. 3 and 4 are summarized by plotting the normalized L^2 -error between the KdV, BBM, Padé and Whitham, respectively, and the Euler solutions as a function of non-dimensional time. Using this quantitative measure of comparison, it appears that the Whitham equation gives the best overall rendition of the free surface dynamics predicted by the Euler equations.

In the center left panels of Figs. 5 and 6, a similar computation with $\delta = 1$, but smaller amplitude is analyzed. Also in these cases, it appears that the Whitham equation gives a good approximation to the corresponding Euler solutions, and in particular, a much better approximation than either the KdV or the BBM equation. The Padé equation also does better than both KdV and BBM equations, but not better than the Whitham equation.

Figs. 5 and 6 show comparisons in several other cases of both positive and negative initial amplitude, and Stokes numbers $\delta = 0.2$, $\delta = 1$ and $\delta = 5$. In most cases, the normalized L^2 -error between the Whitham and Euler solutions is similar or smaller than the errors between the Euler solutions and the other three model equations. However, the Padé equation generally outperforms both the KdV and the BBM equation by some measure.

The only case in this study in which the KdV, BBM and Padé equations outperform the Whitham equation is in the case of

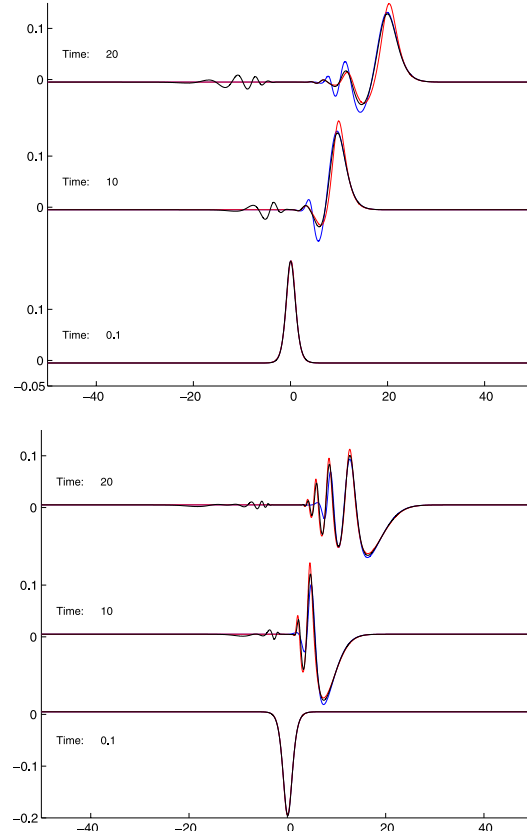


Fig. 4. Wave profiles at three different times: – Euler (black line), – Padé (blue line), – Whitham (red line). Experiment D: $\delta = 1$, $\alpha = 0.2$, $\lambda = \sqrt{5}$. Upper panel: positive case; lower panel: negative case. Horizontal axis: x/h_0 , vertical axis: z/h_0 . Snapshots are given at nondimensional time $t/\sqrt{h_0/g}$.

very long positive initial disturbances. The case when $\delta = 5$ is shown in the lower panels of Fig. 5. However, even in this case, the Whitham equation yields approximations of the Euler solutions which are similar or better than in the case of smaller wavelengths. In addition, in the case of negative initial data, the performance of the Whitham equation is on par with the KdV, BBM and Padé equations in the case when $\delta = 5$ (lower panels of Fig. 5).

5. Conclusion

In this article, the Whitham equation (1) has been studied as an approximate model equation for wave motion at the surface of a perfect fluid. Numerical integration of the equation suggests that broad classes of initial data decompose into individual solitary waves. The wavelength–amplitude ratio of these approximate solitary waves has been studied, and it was found that this ratio can be described by an exponential relation of the form $\frac{a}{h_0} \sim e^{-\kappa(l/h_0)^\nu}$. Using this scaling in the Hamiltonian formulation of the water-wave problem, a system of evolution equations has been derived which contains the exact dispersion relation of the water-wave problem in its linear part. Restricting to one-way propagation, the Whitham equation emerged as a model which combines the usual quadratic nonlinearity with one branch of the exact dispersion relation of the water-wave problem. The performance of the Whitham equation in the approximation of

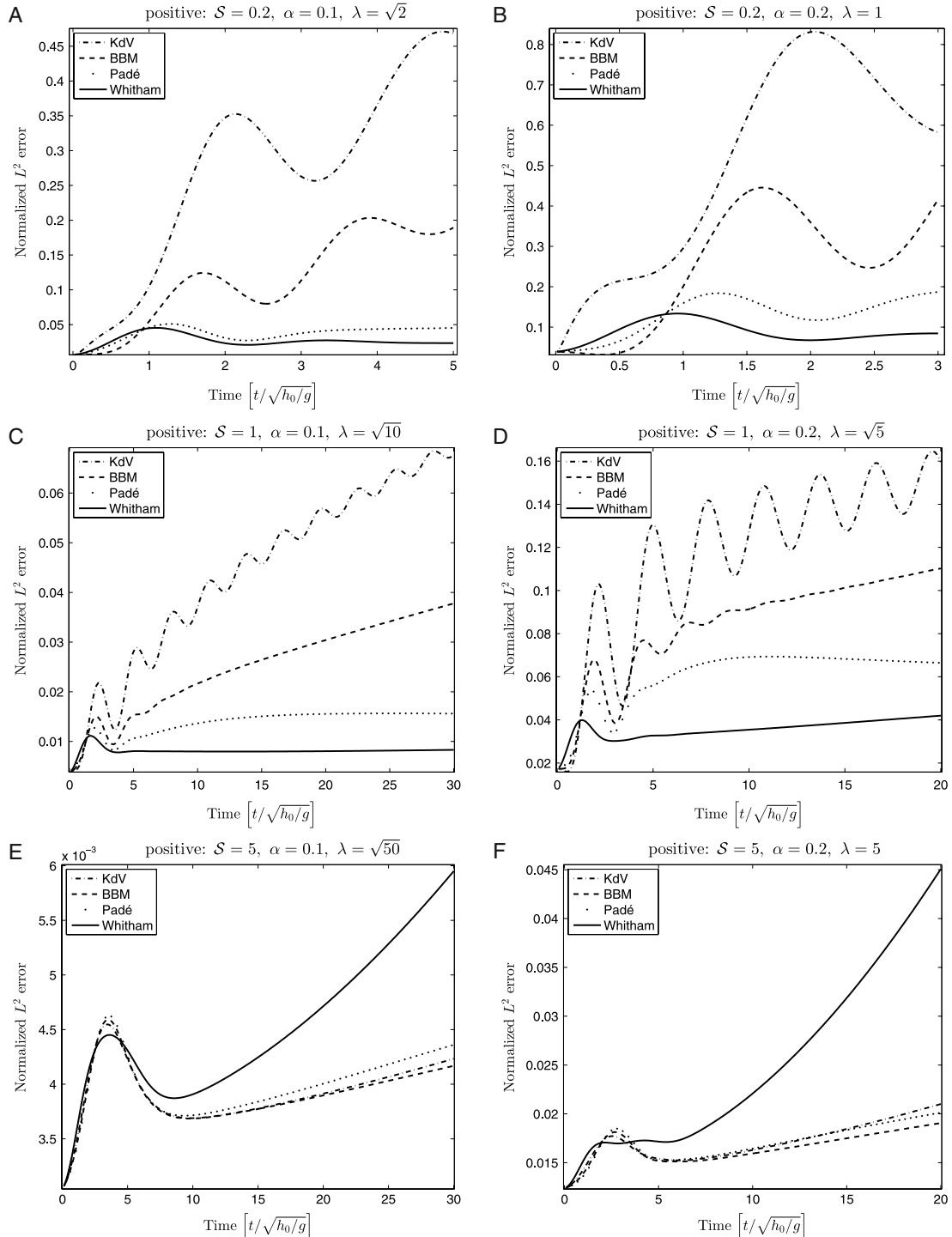


Fig. 5. L^2 errors in approximation of solutions to full Euler equations by different model equations: cases A and B ($\delta = 0.2$), cases C and D ($\delta = 1$), cases E and F ($\delta = 5$), positive.

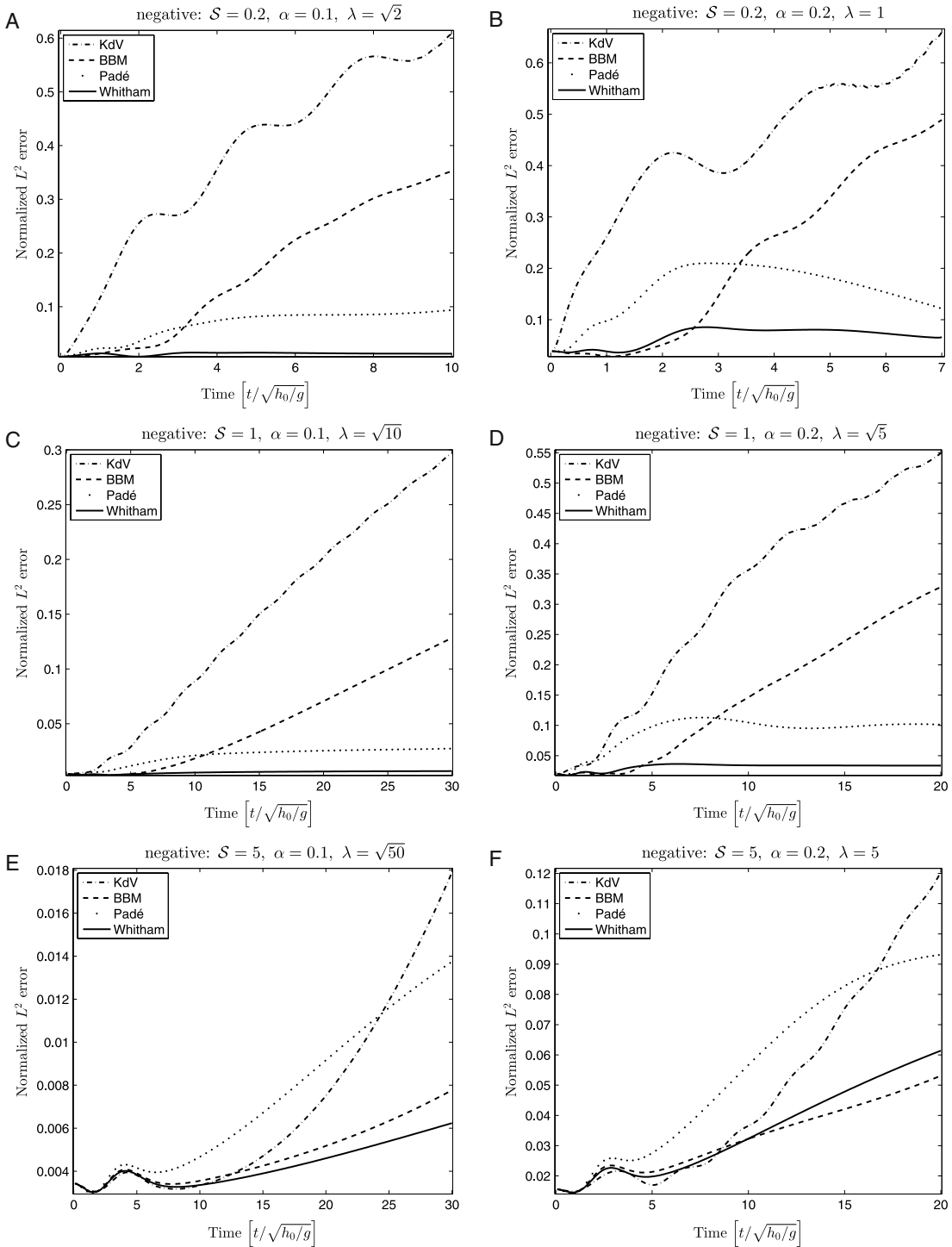


Fig. 6. L^2 errors in approximation of solutions to full Euler equations by different model equations: cases A and B ($\delta = 0.2$), cases C and D ($\delta = 1$), cases E and F ($\delta = 5$), negative.

solutions of the Euler equations free-surface boundary conditions was analyzed, and compared to the performance of the KdV and BBM equations, and to the Padé (2,2) model. It was found that the Whitham equation gives a more faithful representation of the solutions of the Euler equations than either the KdV or the BBM equations, except in the case of very long waves with positive main part. In this last case, the KdV and BBM equations have the upper hand over the Whitham equation. The Padé (2,2) model also outperforms the KdV and BBM equations, but does not quite as well as the Whitham equation for shorter waves and negative disturbances. However, in the case of very long waves with positive main part, the Padé model stays on par with the KdV and BBM equations.

Acknowledgment

This research was supported by the Research Council of Norway (213474/F20).

References

- [1] G.B. Whitham, Variational methods and applications to water waves, Proc. R. Soc. Lond. Ser. A 299 (1967) 6–25.
- [2] M. Ehrnström, M.D. Groves, E. Wahlén, Solitary waves of the Whitham equation – a variational approach to a class of nonlocal evolution equations and existence of solitary waves of the Whitham equation, Nonlinearity 25 (2012) 2903–2936.
- [3] M. Ehrnström, H. Kalisch, Traveling waves for the Whitham equation, Differential Integral Equations 22 (2009) 1193–1210.
- [4] D. Lannes, The Water Waves Problem, in: Mathematical Surveys and Monographs, vol. 188, Amer. Math. Soc, Providence, 2013.
- [5] D. Lannes, J.-C. Saut, Remarks on the full dispersion Kadomtsev-Petviashvili equation, Kinet. Relat. Models 6 (2013) 989–1009.
- [6] C. Klein, J.-C. Saut, A numerical approach to blow-up issues for dispersive perturbations of Burgers' equation, Physica D 295 (2015) 46–65.
- [7] P. Aceves-Sánchez, A.A. Minzoni, P. Panayotaros, Numerical study of a nonlocal model for water-waves with variable depth, Wave Motion 50 (2013) 80–93.
- [8] V.M. Hur, M.A. Johnson, Modulational instability in the Whitham equation of water waves, Stud. Appl. Math. 134 (1) (2015) 120–143.
- [9] N. Sanford, K. Kodama, J.D. Carter, H. Kalisch, Stability of traveling wave solutions to the Whitham equation, Phys. Lett. A 378 (2014) 2100–2107.
- [10] P.G. Drazin, R.S. Johnson, Solitons: an introduction, in: Cambridge Texts in Applied Mathematics, Cambridge University Press, Cambridge, 1989.
- [11] G.B. Whitham, Linear and Nonlinear Waves, Wiley, New York, 1974.
- [12] M. Ablowitz, H. Segur, Solitons and the inverse scattering transform, in: SIAM Studies in Applied Mathematics, vol. 4, SIAM, Philadelphia, 1981.
- [13] W. Craig, C. Sulem, Numerical simulation of gravity waves, J. Comput. Phys. 108 (1993) 73–83.
- [14] V.E. Zakharov, Stability of periodic waves of finite amplitude on the surface of a deep fluid, J. Appl. Mech. Tech. Phys. 9 (1968) 190–194.
- [15] W. Craig, M.D. Groves, Hamiltonian long-wave approximations to the water-wave problem, Wave Motion 19 (1994) 367–389.
- [16] D.H. Peregrine, Calculations of the development of an undular bore, J. Fluid Mech. 25 (1966) 321–330.
- [17] T.B. Benjamin, J.L. Bona, J.J. Mahony, Model equations for long waves in nonlinear dispersive systems, Philos. Trans. R. Soc. Lond., Ser. A 272 (1972) 47–78.
- [18] J.M. Witting, A unified model for the evolution of nonlinear water waves, J. Comput. Phys. 56 (1984) 203–236.
- [19] R. Fetecau, D. Levy, Approximate model equations for water waves, Commun. Math. Sci. 3 (2) (2005) 159–170.
- [20] A.A. Petrov, Variational statement of the problem of liquid motion in a container of finite dimensions, Prikl. Math. Mekh. 28 (1964) 917–922.
- [21] D.P. Nicholls, F. Reitich, A new approach to analyticity of Dirichlet-Neumann operators, Proc. Roy. Soc. Edinburgh Sect. A 131 (2001) 1411–1433.
- [22] W. Craig, P. Guyenne, H. Kalisch, Hamiltonian long-wave expansions for free surfaces and interfaces, Comm. Pure Appl. Math. 58 (2005) 1587–1641.
- [23] M. Ehrnström, H. Kalisch, Global bifurcation for the Whitham equation, Math. Mod. Nat. Phenomena 8 (2013) 13–30.
- [24] B. Fornberg, G.B. Whitham, A numerical and theoretical study of certain nonlinear wave phenomena, Phil. Trans. Roy. Soc. A 289 (1978) 373–404.
- [25] J. De Frutos, J.M. Sanz-Serna, An easily implementable fourth-order method for the time integration of wave problems, J. Comput. Phys. 103 (1992) 160–168.
- [26] L.V. Ovsyannikov, To the shallow water theory foundation, Arch. Mech. 26 (1974) 407–422.
- [27] A.I. Dyachenko, E.A. Kuznetsov, M.D. Spector, V.E. Zakharov, Analytical description of the free surface dynamics of an ideal fluid (canonical formalism and conformal mapping), Phys. Lett. A 221 (1996) 73–79.
- [28] Y.A. Li, J.M. Hyman, W. Choi, A numerical study of the exact evolution equations for surface waves in water of finite depth, Stud. Appl. Math. 113 (2004) 303–324.
- [29] W. Choi, R. Camassa, Exact evolution equations for surface waves, J. Eng. Mech. 125 (1999) 756–760.
- [30] P. Milewski, J.-M. Vanden-Broeck, Z. Wang, Dynamics of steep two-dimensional gravity-capillary solitary waves, J. Fluid Mech. 664 (2010) 466–477.
- [31] D. Mitsotakis, D. Dutykh, J.D. Carter, On the nonlinear dynamics of the traveling-wave solutions of the Serre equations (2014) submitted for publication, <http://arxiv.org/abs/1404.6725>.
- [32] J.L. Hammack, H. Segur, The Korteweg-de Vries equation and water waves. Part 2. Comparison with experiments, J. Fluid Mech. 65 (1974) 289–314.

Paper B

3.2 Paper title

List of authors

Physical Review B, **76**, 035303 (2007)

THE WHITHAM EQUATION WITH SURFACE TENSION

EVGUENI DINVAY, DAULET MOLDABAYEV, DENYS DUTYKH, AND HENRIK KALISCH

ABSTRACT. The Whitham equation was proposed as an alternate model equation for the simplified description of uni-directional wave motion at the surface of an inviscid fluid. As the Whitham equation incorporates the full linear dispersion relation of the water wave problem, it is thought to provide a more faithful description of shorter waves of small amplitude than traditional long wave models such as the KdV equation. In this work, we derive the Whitham equation from the Hamiltonian theory of surface water waves while taking into account surface tension. It is shown numerically that in various scaling regimes the Whitham equation gives a more accurate approximation of the free-surface problem for the Euler system than other models like the KdV, BBM or Kawahara equation. Only in the case of very long waves with positive polarity do the KdV and Kawahara equations outperform the Whitham equation with surface tension.

1. INTRODUCTION

In its simplest form, the water-wave problem concerns the flow of an incompressible inviscid fluid with a free surface over a horizontal impenetrable bed. In this situation, the fluid flow is described by the Euler equations with appropriate boundary conditions, and the dynamics of the free surface are of particular interest in the solutions of this problem.

There are a number of model equations which allow the approximate description of the evolution of the free surface without having to provide a complete solution of the fluid flow below the surface. In the present contribution, interest is focused on the derivation and evaluation of a non-local water-wave model known as the Whitham equation. We extend here the results of the work [26] to the case where surface tension is taken into account. The model equation under study is written as

$$\eta_t + W\eta_x + \frac{3}{2}\eta\eta_x = 0, \quad (1.1)$$

where the convolution kernel of the operator $W\eta_x = w(-i\partial_x)\eta_x = (\mathcal{F}^{-1}w) * \eta_x$ is given in terms of the Fourier transform by

$$w(\xi) = \sqrt{(1 + \varkappa\xi^2) \frac{\tanh(\xi)}{\xi}}. \quad (1.2)$$

Here it is assumed that the variables are suitably normalized so that the gravitational acceleration, the undisturbed depth of the fluid and the density are all unity. The surface fluid tension is included here by means of the capillarity parameter \varkappa which is the inverse of the Bond number. The convolution can be thought of as a Fourier multiplier operator, and (1.2) represents the Fourier symbol of the operator. It is also convenient from the analytical point of view to regard the Whitham operator $W = w(-i\partial_x)$ as an integral with respect to the spectral measure of the self-adjoint operator $-i\partial_x$ in $L^2(\mathbb{R})$. Thus after linearisation (1.1) can be considered as a Schrödinger equation with the self-adjoint

Date: November 7, 2016.

operator $-i\partial_x w(-i\partial_x)$. Indeed, introducing operator $D = -i\partial_x$ one may rewrite (1.1) as

$$i\eta_t = Dw(D)\eta + \frac{3}{4}D\eta^2.$$

From this point of view, for example, one may deduce straight away that for any real valued solution $\eta \in C^1(\mathbb{R}, L^2(\mathbb{R}))$ of this equation the L^2 -norm does not depend on time.

The Whitham equation was proposed by Whitham [32] as an alternative to the well known Korteweg-de Vries (KdV) equation

$$\eta_t + \eta_x + \frac{3}{2}\eta\eta_x - \frac{1}{2}\left(\varkappa - \frac{1}{3}\right)\eta_{xxx} = 0. \quad (1.3)$$

Provided $\varkappa < 1/3$ one may rescale x and t by $\sqrt{1-3\varkappa}$ and arrive at the equation

$$\eta_t + \eta_x + \frac{3}{2}\eta\eta_x + \frac{1}{6}\eta_{xxx} = 0.$$

Thus it is apparent that small capillary effect do not add anything new to the KdV model. However, when \varkappa is near $1/3$ one cannot expect that this model be applicable. To describe surface waves in such a situation, one may use instead the fifth-order-model equation

$$\eta_t + \eta_x + \frac{3}{2}\eta\eta_x - \frac{1}{2}\left(\varkappa - \frac{1}{3}\right)\eta_{xxx} + \frac{1}{360}(19 - 30\varkappa - 45\varkappa^2)\eta_{xxxxx} = 0. \quad (1.4)$$

In our numerical experiments we use $\varkappa = 1/3$, so that the equation reduces to what is known as the Kawahara equation [3, 6, 20], which has the following form:

$$\eta_t + \eta_x + \frac{3}{2}\eta\eta_x + \frac{1}{90}\eta_{xxxxx} = 0.$$

The validity of the KdV and Kawahara equations can be described in the terms of the Stokes number $\mathcal{S} = \alpha\lambda^2$ where $\alpha = a/h_0$ and λ/h_0 represent a prominent amplitude and a characteristic wavelength of the wave field respectively. The KdV equation is known to be a good model for water waves if the amplitude of the waves is small and the wavelength is large when compared to the undisturbed depth, and if in addition, the two non-dimensional quantities α and $1/\lambda^2$ are of similar size which means $\mathcal{S} \sim 1$. With the same requirement and \varkappa near $1/3$ the Kawahara equation gives better results for waves where capillarity is important. Another alternative model to the KdV equation (1.3) known as the BBM equation was put forward in [29] and studied in depth in [4]. That one with the capillarity \varkappa has the form

$$\eta_t + \eta_x + \frac{3}{2}\eta\eta_x + \frac{1}{2}\left(\varkappa - \frac{1}{3}\right)\eta_{xxt} = 0. \quad (1.5)$$

The linearized dispersion relation of this equation is not an exact match to the dispersion relation of the full water-wave problem, but it is much closer than the KdV equation in the case when $\varkappa < 1/3$, and it might also be expected that this equation may be able to model shorter waves more successfully than the KdV equation. However, the domain of its applicability is $\mathcal{S} \sim 1$, that coincides with the corresponding restrictions of the KdV model [4]. One may also notice that (1.5) can also be scaled to the equation without capillarity in the same way as (1.3) providing capillarity \varkappa is small.

Both KdV and Kawahara equations are generally believed to approximate very long waves quite well, but one notorious problem with these equations is that they do not model accurately the dynamics of shorter waves. Recognizing this shortcoming of the KdV equation, Whitham proposed to use the same nonlinearity as the KdV equation, but coupled with a linear term which mimics the linear dispersion relation of the full

water-wave problem. Thus, at least in theory, the Whitham equation can be expected to yield a description of the dynamics of shorter waves which is closer to the governing Euler equations. The Whitham equation (1.1) has been studied from a number of vantage points during recent years. In particular, the existence of traveling and solitary waves has been studied [1, 13, 14, 15]. Well posedness of a similar equation was investigated in [22]. Moreover, it has been shown in [18, 19, 31] that periodic solutions of equation (1.1) feature modulational instability for short enough waves in a similar way as small-amplitude periodic wave solutions of the water-wave problem. The performance of the Whitham equation in the description of surface water waves has been investigated in [5] in the steady case without surface tension. However, it appears that no study of the performance of the Whitham equation in the presence of capillarity has been done.

In the present note, we give an asymptotic derivation of the Whitham equation as a model for surface water waves, giving close consideration to the influence of the surface tension. The derivation proceeds by examining the Hamiltonian formulation of the water-wave problem due to Zhakarov, Craig and Sulem [34, 10]. This approach is similar to the method of [8]. However, our consideration is not constrained heavily by any particular scalar regime. Firstly, a corresponding Whitham system is derived, and then the Whitham equation is found by restricting the system to one-way propagation. Secondly, we derive different models from the Whitham equation and point out the corresponding domains of their applicability.

Finally, a numerical comparison of modeling properties of the KdV, Kawahara and Whitham equations is given with respect to the Euler system.

2. EULER SYSTEM AND ITS HAMILTONIAN

The surface water-wave problem is generally described by the Euler equations with no-flow conditions at the bottom, and kinematic and dynamic boundary conditions at the free surface. Assuming weak transverse effects, the unknowns are the surface elevation $\eta(x, t)$, the horizontal and vertical fluid velocities $u_1(x, z, t)$ and $u_2(x, z, t)$, respectively, and the pressure $P(x, z, t)$. If the assumption of irrotational flow is made, then a velocity potential $\phi(x, z, t)$ can be used. Taking the undisturbed depth $h_0 = 1$ as a unit of distance, and the parameter $\sqrt{h_0/g} = 1$ as a unit of time, the problem may be posed on a domain $\{(x, z) \in \mathbb{R}^2 \mid -1 < z < \eta(x, t)\}$ which extends to infinity in the positive and negative x -direction. Due to the incompressibility of the fluid, the potential then satisfies the Laplace's equation in this domain. The fact that the fluid cannot penetrate the bottom is expressed by a homogeneous Neumann boundary condition at the flat bottom. Thus we have

$$\begin{aligned}\phi_{xx} + \phi_{zz} &= 0 \quad \text{in} \quad -1 < z < \eta(x, t) \\ \phi_z &= 0 \quad \text{on} \quad z = -1.\end{aligned}$$

The pressure is eliminated with help of the Bernoulli equation, and the free-surface boundary conditions are formulated in terms of the potential φ and the surface displacement η by

$$\left. \begin{aligned}\eta_t + \phi_x \eta_x - \phi_z &= 0, \\ \phi_t + \frac{1}{2}(\phi_x^2 + \phi_z^2) + \eta - \kappa \eta_{xx} (1 + \eta_x^2)^{-3/2} &= 0,\end{aligned}\right\} \text{on } z = \eta(x, t).$$

The first equation represents the definition of the fluid velocity with respect to the Euler coordinates. The second one is the Bernoulli equation with the capillary term.

The total energy of the system is given by the sum of the kinetic energy, the potential energy and the surface tension energy, and normalized in such a way that the total energy

is zero when no wave motion is present at the surface. Accordingly the Hamiltonian function for this problem is

$$H = \int_{\mathbb{R}} \int_0^\eta z dz dx + \int_{\mathbb{R}} \int_{-1}^\eta \frac{1}{2} |\nabla \phi|^2 dz dx + \varkappa \int_{\mathbb{R}} \frac{\eta_x^2}{1+\sqrt{1+\eta_x^2}} dx.$$

Defining the trace of the potential at the free surface as $\Phi(x, t) = \phi(x, \eta(x, t), t)$, one may integrate in z in the first integral and use the divergence theorem on the second integral in order to arrive at the formulation

$$H = \int_{\mathbb{R}} \left[\frac{1}{2} \eta^2 + \frac{1}{2} \Phi G(\eta) \Phi + \varkappa \frac{\eta_x^2}{1+\sqrt{1+\eta_x^2}} \right] dx. \quad (2.1)$$

This is the Hamiltonian of the water wave problem with surface tension as for instance found in [2], and written in terms of the Dirichlet-Neumann operator $G(\eta)$. As shown in [27], the Dirichlet-Neumann operator is analytic in a certain sense, and can be expanded as a power series as

$$G(\eta)\Phi = \sum_{j=0}^{\infty} G_j(\eta)\Phi.$$

In order to proceed, we need to understand the first few terms in this series. As shown in [10] and [8], the first two terms in this series can be written with the help of the operator $D = -i\partial_x$ as

$$G_0(\eta) = D \tanh(D), \quad G_1(\eta) = D\eta D - D \tanh(D)\eta D \tanh(D).$$

Note that it can be shown that the terms $G_j(\eta)$ for $j \geq 2$ are of quadratic or higher-order in η , and will therefore not be needed in the following analysis.

It will be convenient for the present purpose to formulate the Hamiltonian in terms of the dependent variable $u = \Phi_x$. This new variable is proportional to the velocity of the fluid tangential to the surface. More precisely $u = \varphi_x + \eta_x \varphi_z = \varphi_\tau \sqrt{1+\eta_x^2}$ where φ_τ is exactly the tangential velocity component to the surface. To this end, we define the operator \mathcal{K} by

$$G(\eta) = D\mathcal{K}(\eta)D.$$

As was the case with $G(\eta)$, the operator $\mathcal{K}(\eta)$ can also be expanded in a Taylor series with respect to powers of η and η_x as

$$\mathcal{K}(\eta) = \sum_{j=0}^{\infty} \mathcal{K}_j(\eta), \quad \mathcal{K}_j(\eta) = D^{-1} G_j(\eta) D^{-1}.$$

In particular, note that $\mathcal{K}_0 = \tanh D/D$ and $\mathcal{K}_1 = \eta - \tanh D(\eta \tanh D)$. After integrating by parts the Hamiltonian can be expressed as

$$H = \int_{\mathbb{R}} \left[\frac{1}{2} \eta^2 + \frac{1}{2} u \mathcal{K}(\eta) u + \varkappa \frac{\eta_x^2}{1+\sqrt{1+\eta_x^2}} \right] dx. \quad (2.2)$$

The following analysis has the formal character of long-wave approximation. Consider a wave-field having a characteristic non-dimensional wavelength λ and a characteristic non-dimensional amplitude α . We also introduce the small parameter $\mu = \frac{1}{\lambda}$. To obtain different approximations of the discussed problem the amplitude α is considered as a function of wave-number μ . Its behaviour at small wave-numbers defines different scaling regimes. The long-wave approximation means the scale $\eta = O(\alpha)$, $u = O(\alpha)$ and $D = -i\partial_x = O(\mu)$ where $\alpha = \alpha(\mu)$ depends on the small parameter μ . Now the Hamiltonian (2.2) may be simplified as follows

$$H = H_g + H_c + O(\mu^2 \alpha^4) \quad (2.3)$$

with the gravity term

$$H_g = \frac{1}{2} \int_{\mathbb{R}} \left[\eta^2 + u \frac{\tanh D}{D} u + \eta u^2 - u \tanh D (\eta \tanh D u) \right] dx \quad (2.4)$$

and the capillary part

$$H_c = \varkappa \int_{\mathbb{R}} \frac{\eta_x^2 dx}{1 + \sqrt{1 + \eta_x^2}} = \frac{\varkappa}{2} \int_{\mathbb{R}} \eta_x^2 dx + O(\mu^4 \alpha^4). \quad (2.5)$$

Before we continue with derivation of the Whitham equation we prove the following lemma about integration by parts, which is certainly well-known and we add it here only for completeness.

Lemma 2.1. *Let f, g be real-valued square integrable functions on real axis \mathbb{R} . Regard $D = -i\partial_x$ as self-adjoint on $L^2(\mathbb{R}, \mathbb{C})$ and a real-valued function φ that is measurable and almost everywhere finite with respect to Lebesgue measure. If f, g lie in the domain of the operator $\varphi(D)$ then*

$$\int F\varphi(D)g = \int G\varphi(-D)f$$

Proof. It is given two proofs below. The first one is to regard $\varphi(D) = (\mathcal{F}^{-1}\varphi)*$ as the operator of convolution in the sense of distribution theory

$$\begin{aligned} \int f\varphi(D)g &= \int f(\xi)(\mathcal{F}^{-1}\varphi)(\xi - x)g(x)dxd\xi = \\ &= \int f(\xi)(\mathcal{F}^{-1}\varphi \circ (-id))(x - \xi)g(x)dxd\xi = \int g\varphi(-D)f. \end{aligned}$$

The second proof is to represent $\varphi(D) = \int \varphi dE$ as the integral with respect to spectral measure E of the operator D . The corresponding projector of the interval (α, β) is the convolution with the function $e_{(\alpha, \beta)}(x) = \frac{1}{2\pi ix}(e^{i\beta x} - e^{i\alpha x})$. So the replacement of f and g changes the corresponding spectral complex measure of intervals as follows

$$\begin{aligned} \mu_{f,g}(\alpha, \beta) &= (E(\alpha, \beta)f, g) = \int e_{(\alpha, \beta)}(x - y)f(y)g(x)dxdy = \\ &= \int e_{(-\beta, -\alpha)}(y - x)f(y)g(x)dxdy = \mu_{g,f}(-\beta, -\alpha) \end{aligned}$$

which implies the statement of the lemma

$$\int f\varphi(D)g = \int \varphi(x)d\mu_{g,f}(x) = \int \varphi(-x)d\mu_{f,g}(x) = \int g\varphi(-D)f.$$

□

3. DERIVATION OF THE WHITHAM TYPE EVOLUTION SYSTEM

The water-wave problem can be rewritten as a Hamiltonian system using the variational derivatives of H . Making reference to [8, 9] note that the pair (η, Φ) represents the canonical variables for the Hamiltonian function (2.1). However, it is more common to write the equations of motion in the fluid dynamics of free surface in terms of η and $u = \Phi_x$. The transformation $(\eta, \Phi) \mapsto (\eta, u)$ is associated with the Jacobian

$$\frac{\partial(\eta, u)}{\partial(\eta, \Phi)} = \begin{pmatrix} 1 & 0 \\ 0 & \partial_x \end{pmatrix}.$$

Thus in terms of η and u the Hamiltonian equations have the form

$$\eta_t = -\partial_x \frac{\delta H}{\delta u}, \quad u_t = -\partial_x \frac{\delta H}{\delta \eta} \quad (3.1)$$

that is not canonical since the associated structure map $J_{\eta,u}$ is symmetric:

$$J_{\eta,u} = \begin{pmatrix} \frac{\partial(\eta, u)}{\partial(\eta, \Phi)} \\ \frac{\partial(\eta, u)}{\partial(\eta, \Phi)} \end{pmatrix} \begin{pmatrix} 0 & 1 \\ -1 & 0 \end{pmatrix} \begin{pmatrix} \frac{\partial(\eta, u)}{\partial(\eta, \Phi)} \\ \frac{\partial(\eta, u)}{\partial(\eta, \Phi)} \end{pmatrix}^* = \begin{pmatrix} 0 & -\partial_x \\ -\partial_x & 0 \end{pmatrix}.$$

We now proceed to derive a system of equations which is similar to the Whitham equation (1.1), but allows bi-directional wave propagation. This system will be a stepping stone on the way to a derivation of (1.1), but may also be of independent interest. The variational derivative $\delta H_g / \delta u$ is defined by means of any real-valued square integrable function h as follows

$$\begin{aligned} \int_{\mathbb{R}} \frac{\delta H_g}{\delta u}(x) h(x) dx &= d_u H_g h = \left. \frac{d}{d\tau} \right|_{\tau=0} H_g(u + \tau h, \eta) = \int_{\mathbb{R}} u \eta h dx + \\ &+ \frac{1}{2} \int_{\mathbb{R}} \left[h \frac{\tanh D}{D} u + u \frac{\tanh D}{D} h - h \tanh D (\eta \tanh Du) - u \tanh D (\eta \tanh Dh) \right] dx. \end{aligned}$$

Making use of integration by parts described in Lemma 2.1 one obtains

$$\frac{\delta H_g}{\delta u} = \frac{\tanh D}{D} u + \eta u - \tanh D (\eta \tanh Du) = \frac{\tanh D}{D} u + \eta u + O(\mu^2 \alpha^2)$$

and in the same way

$$\frac{\delta H_g}{\delta \eta} = \eta + \frac{1}{2} u^2 + \frac{1}{2} (\tanh Du)^2 = \eta + \frac{1}{2} u^2 + O(\mu^2 \alpha^2).$$

These variational derivatives were also obtained by Moldabayev and Kalisch [26]. The capillary part H_c defined by (2.5) gives the pressure P on the surface

$$\frac{\delta H_c}{\delta \eta} = -\varkappa \frac{\eta_{xx}}{(1 + \eta_x^2)^{\frac{3}{2}}} = -\varkappa \eta_{xx} + O(\mu^4 \alpha^3).$$

At last the Hamilton system (3.1) is simplified to the Whitham system

$$\eta_t = -\frac{\tanh D}{D} u_x - (\eta u)_x + \tanh D (\eta \tanh Du)_x + O(\mu^3 \alpha^3), \quad (3.2)$$

$$u_t = -\eta_x - uu_x - (\tanh Du) \tanh Du_x + \varkappa \eta_{xxx} + O(\mu^3 \alpha^3) \quad (3.3)$$

which is in line with the system obtained in [26]

$$\begin{aligned} \eta_t &= -\frac{\tanh D}{D} u_x - (\eta u)_x + O(\mu^3 \alpha^2), \\ u_t &= -\eta_x - uu_x + \varkappa \eta_{xxx} + O(\mu^3 \alpha^2). \end{aligned}$$

4. DERIVATION OF WHITHAM TYPE EVOLUTION EQUATIONS

It turns out that the Whitham system (3.2), (3.3) might be rewritten as a system of two independent equations by further simplification. More precisely, they will be independent with respect to the linear approximation of that system. For this purpose we need to separate solutions corresponding to waves moving in other directions. In order to derive the Whitham equation for uni-directional wave propagation, it is important to

understand how one-way propagation works in the Whitham system (3.2), (3.3). Regard the linearisation of this system

$$\eta_t + \frac{\tanh D}{D} u_x = 0, \quad (4.1)$$

$$u_t + (1 + \varkappa D^2) \eta_x = 0. \quad (4.2)$$

Regarding solutions of this linear system in the wave form

$$\eta(x, t) = A e^{i\xi x - i\omega t}, \quad u(x, t) = B e^{i\xi x - i\omega t}$$

gives rise to the matrix equation

$$\begin{pmatrix} -\omega & \tanh \xi \\ \xi + \varkappa \xi^3 & -\omega \end{pmatrix} \begin{pmatrix} A \\ B \end{pmatrix} = \begin{pmatrix} 0 \\ 0 \end{pmatrix}.$$

This equation has a non-trivial solution, provided its determinant equals zero, so that $\omega^2 - (\xi + \varkappa \xi^3) \tanh \xi = 0$. Defining the phase speed as $c = \omega(\xi)/\xi$ one obtains the dispersion relation

$$c^2(\xi) = (1 + \varkappa \xi^2) \frac{\tanh \xi}{\xi}$$

which coincides, up to the sign of c , with Whitham dispersion relation (1.2). Obviously, the choice $c > 0$ corresponds to right-going wave solutions of the linear system (4.1), (4.2). And the phase speed $c < 0$ gives left-going waves. To split up these two kinds of waves we regard the following transformation of variables

$$r = \frac{1}{2}(\eta + Ku), \quad s = \frac{1}{2}(\eta - Ku). \quad (4.3)$$

It is supposed that K is an invertible operator, namely an invertible function of the differential operator D . The inverse transformation has the form

$$\eta = r + s, \quad u = K^{-1}(r - s). \quad (4.4)$$

The question arises whether it is possible to choose such operator K that r and s correspond to right- and left-going waves, respectively. After applying the transformation (4.4) to the linear system (4.1), (4.2) one arrives to the system

$$\begin{aligned} r_t + \partial_x(A(D, K)r + B(D, K)s) &= 0, \\ s_t - \partial_x(A(D, K)s + B(D, K)r) &= 0 \end{aligned}$$

where operators A and B depend on D and K as follows

$$A = \frac{1}{2} \left((1 + \varkappa D^2)K + \frac{\tanh D}{D} K^{-1} \right), \quad B = \frac{1}{2} \left((1 + \varkappa D^2)K - \frac{\tanh D}{D} K^{-1} \right).$$

So to achieve independence of the obtained two equations we need to choose the transformation K in the way $B(D, K) = 0$, so that

$$K = \sqrt{\frac{1}{1 + \varkappa D^2} \cdot \frac{\tanh D}{D}} \quad (4.5)$$

whish leads to the two independent Whitham equations

$$r_t + \partial_x W r = 0, \quad (4.6)$$

$$s_t - \partial_x W s = 0 \quad (4.7)$$

where the Whitham operator $W = w(D) = A(D, K)$ was introduced at the beginning of the paper by (1.2). If we again regard the wave solutions $r(x, t) = \exp(i\xi x - i\omega_r t)$ and $s(x, t) = \exp(i\xi x - i\omega_s t)$ then we conclude that the first equation (4.6) describes waves

moving to the right with the phase velocity $c_r = \omega_r/\xi = w(\xi)$ and the second equation (4.7) corresponds to the left-going waves with $c_s = \omega_s/\xi = -w(\xi)$.

Now we regard the Hamiltonian (2.2) as a functional of r and s with the same long-wave approximation as before (2.3) where obviously $r = O(\alpha)$ and $s = O(\alpha)$. The unperturbed Hamiltonian part (2.4) is

$$H_g = \frac{1}{2} \int_{\mathbb{R}} \left[(r+s)^2 + (K^{-1}(r-s)) \frac{\tanh D}{D} K^{-1}(r-s) + (r+s)(K^{-1}(r-s))^2 - (K^{-1}(r-s)) \tanh D((r+s) \tanh D K^{-1}(r-s)) \right] dx \quad (4.8)$$

and the surface tension adding (2.5) is

$$H_c = \frac{\varkappa}{2} \int_{\mathbb{R}} (r+s)_x^2 dx + O(\mu^4 \alpha^4). \quad (4.9)$$

According to the transformation theory detailed in [9], due to the changing of variables (4.3) or (4.4), the structure map changes to

$$J_{r,s} = \left(\frac{\partial(r,s)}{\partial(\eta,u)} \right) J_{\eta,u} \left(\frac{\partial(r,s)}{\partial(\eta,u)} \right)^* = \begin{pmatrix} -\frac{1}{2} \partial_x K & 0 \\ 0 & \frac{1}{2} \partial_x K \end{pmatrix}.$$

The corresponding Hamiltonian system has the form

$$r_t + \partial_x \left(\frac{K \delta H}{2 \delta r} \right) = 0, \quad s_t - \partial_x \left(\frac{K \delta H}{2 \delta s} \right) = 0. \quad (4.10)$$

These equations are equivalent to (3.1). However, solutions $r(x,t)$ and $s(x,t)$ are the displacements going right and left, respectively, when a solution $u(x,t)$, representing the tangential velocity component up to the curvature multiplier, might not be imagined so easy. As above we calculate the Gâteaux derivative of H_g given by (4.8) with respect to r at a real-valued square integrable function

$$\begin{aligned} \int_{\mathbb{R}} \frac{\delta H_g}{\delta r}(x) h(x) dx &= d_r H_g h = \frac{d}{d\tau} \Big|_{\tau=0} H_g(r + \tau h, s) = \int (r+s) h + \\ &+ \frac{1}{2} \int (K^{-1} h) \frac{\tanh D}{D} K^{-1}(r-s) + \frac{1}{2} \int (K^{-1}(r-s)) \frac{\tanh D}{D} K^{-1} h + \\ &+ \frac{1}{2} \int h (K^{-1}(r-s))^2 + \int (r+s)(K^{-1}(r-s)) K^{-1} h - \\ &- \frac{1}{2} \int (K^{-1} h) \tanh D((r+s) \tanh D K^{-1}(r-s)) - \\ &- \frac{1}{2} \int (K^{-1}(r-s)) \tanh D(h \tanh D K^{-1}(r-s)) - \\ &- \frac{1}{2} \int (K^{-1}(r-s)) \tanh D((r+s) \tanh D K^{-1} h). \end{aligned}$$

Integrating by parts as in Lemma 2.1 and taking into account that functions $\tanh D$ is odd while K is even (4.5) with respect to D one can obtain $\delta H_g/\delta r$, and in the similar way $\delta H_c/\delta r$, $\delta H_g/\delta s$, $\delta H_c/\delta s$. Thus as a result

$$\begin{aligned} \frac{K \delta H}{2 \delta r} &= W r + \frac{1}{4} K (K^{-1}(r-s))^2 + \frac{1}{2} (r+s) K^{-1}(r-s) + \\ &+ \frac{1}{4} K (\tanh D K^{-1}(r-s))^2 - \frac{1}{2} \tanh D((r+s) \tanh D K^{-1}(r-s)) + O(\mu^2 \alpha^3) \quad (4.11) \end{aligned}$$

and

$$\begin{aligned} \frac{K}{2} \frac{\delta H}{\delta s} &= Ws + \frac{1}{4} K(K^{-1}(r-s))^2 - \frac{1}{2}(r+s)K^{-1}(r-s) + \\ &+ \frac{1}{4} K(\tanh DK^{-1}(r-s))^2 + \frac{1}{2} \tanh D((r+s)\tanh DK^{-1}(r-s)) + O(\mu^2\alpha^3) \end{aligned} \quad (4.12)$$

together with (4.10) are the Whitham system describing the displacement $\eta(x, t)$ in terms of waves going right and left. This system is entirely equivalent to (3.2), (3.3) and at the same time gives rise to solutions with more clear physical meaning. Another useful property of this system is that it can be enough to regard only one equation if we are allowed to neglect the waves going to a particular direction. More precisely, regarding only right-going waves leads to

$$\begin{aligned} \frac{K}{2} \frac{\delta H}{\delta r} &= Wr + \frac{1}{4} K(K^{-1}r)^2 + \frac{1}{2} r K^{-1}r + \\ &+ \frac{1}{4} K(\tanh DK^{-1}r)^2 - \frac{1}{2} \tanh D(r \tanh DK^{-1}r) + O(\alpha|s|) + O(\mu^2\alpha^3) \end{aligned} \quad (4.13)$$

and only left-going waves gives

$$\begin{aligned} \frac{K}{2} \frac{\delta H}{\delta s} &= Ws + \frac{1}{4} K(K^{-1}s)^2 + \frac{1}{2} s K^{-1}s + \\ &+ \frac{1}{4} K(\tanh DK^{-1}s)^2 - \frac{1}{2} \tanh D(s \tanh DK^{-1}s) + O(\alpha|r|) + O(\mu^2\alpha^3). \end{aligned} \quad (4.14)$$

As one can see these expressions are identical up to discarded parts. Equality (4.13) together with the first equation of (4.10) corresponds to the Whitham equation describing right-going surface waves. Equality (4.14) together with the second equation of (4.10) corresponds to the Whitham equation describing left-going surface waves. Further simplifications can be made by studying concrete regimes $\alpha(\mu)$. As a matter of fact, examples of behaviour $\alpha(\mu)$ at small μ that we regard below need less accurate asymptotic. So that operators K and $\tanh D$ can still be simplified by taking into account $D = O(\mu)$ in Equality (4.13) as follows

$$\begin{aligned} \frac{K}{2} \frac{\delta H}{\delta r} &= Wr + \frac{3}{4} r^2 + \frac{1}{4} \left(\varkappa - \frac{5}{3} \right) r D^2 r - \frac{1}{4} \left(\varkappa + \frac{4}{3} \right) (Dr)^2 + \\ &+ O(\mu^4\alpha^2) + O(\alpha|r|) + O(\mu^2\alpha^3). \end{aligned} \quad (4.15)$$

It is in line with [26] for liquids without surface tension $\varkappa = 0$. There is the same expression for the other variational derivative with replacement r by s .

4.1. Linear approximation. Let r and s be of the same order and $\alpha = o(1)$ as $\mu \rightarrow 0$. Then (4.13), (4.14) are simplified to

$$\frac{K}{2} \frac{\delta H}{\delta r} = Wr(1 + o(1)), \quad \frac{K}{2} \frac{\delta H}{\delta s} = Ws(1 + o(1))$$

that together with (4.10) represent two independent linear equations. We again arrived to (4.6), (4.7). This is the case when we do not have enough information about order relation between right- and left-going waves.

4.2. The shallow-water scaling regime. Let $\alpha = O(1)$ as $\mu \rightarrow 0$. Assume also that left-going waves can be discarded $s = o(1)$. In this case operators W can also be simplified by taking into account $D = O(\mu)$. Expression (4.15) becomes

$$\frac{K}{2} \frac{\delta H}{\delta r} = r + \frac{3}{4} r^2 + o(1)$$

which leads to the shallow-water equation

$$r_t + r_x + \frac{3}{2} rr_x = o(\mu).$$

4.3. The Boussinesq scaling regime. Let $\alpha = O(\mu^2)$ and $s = o(\mu^2)$ as $\mu \rightarrow 0$. Expression (4.15) becomes

$$\frac{K}{2} \frac{\delta H}{\delta r} = Wr + \frac{3}{4} r^2 + o(\mu^4)$$

that can be simplified further by two different ways

$$W = 1 + \frac{1}{2} \left(\varkappa - \frac{1}{3} \right) D^2 + O(\mu^4) = \left(1 - \frac{1}{2} \left(\varkappa - \frac{1}{3} \right) D^2 \right)^{-1} + O(\mu^4).$$

The first equality leads to the KdV equation

$$r_t + r_x - \frac{1}{2} \left(\varkappa - \frac{1}{3} \right) r_{xxx} + \frac{3}{2} rr_x = o(\mu^5).$$

The second equality gives rise to the BBM equation

$$r_t + r_x + \frac{1}{2} \left(\varkappa - \frac{1}{3} \right) r_{xxt} + \frac{3}{2} rr_x = o(\mu^5).$$

4.4. The Padé (2,2) approximation. Suppose $\alpha = O(\mu^4)$ and $s = o(\mu^4)$ as $\mu \rightarrow 0$. Expression (4.15) becomes

$$\frac{K}{2} \frac{\delta H}{\delta r} = Wr + \frac{3}{4} r^2 + o(\mu^8)$$

that can be simplified further provided $\varkappa \neq 1/3$ by the way

$$W = \frac{1 + aD^2}{1 + bD^2} + O(\mu^6)$$

where constants a and b depend on \varkappa as follows

$$a(\varkappa) = \frac{3 + 10\varkappa - 45\varkappa^2}{20(1 - 3\varkappa)},$$

$$b(\varkappa) = \frac{19 - 30\varkappa - 45\varkappa^2}{60(1 - 3\varkappa)}.$$

The corresponding equation

$$r_t + r_x - a(\varkappa)r_{xxx} - b(\varkappa)r_{xxt} + \frac{3}{2} rr_x = o(\mu^9).$$

As one can see the order of this differential equation is the same as the order of KdV or BBM, meanwhile the Padé approximation is more accurate. In the case $\varkappa = 1/3$ one has to use the usual Taylor approximation

$$W = 1 + \frac{1}{2} \left(\varkappa - \frac{1}{3} \right) D^2 + \frac{1}{360} (19 - 30\varkappa - 45\varkappa^2) D^4 + O(\mu^6)$$

Experiment	Stokes number \mathcal{S}	Amplitude α	Wavelength λ
A	1	0.1	$\sqrt{10}$
B	1	0.2	$\sqrt{5}$
C	10	0.1	10
D	10	0.2	$\sqrt{50}$
E	0.1	0.1	1
F	0.1	0.2	$\sqrt{1/2}$

TABLE 1. Summary of the Stokes number, nondimensional wavelength, nondimensional amplitude of the initial data used in the numerical experiments.

which gives rise to the equation of fifth order

$$r_t + r_x - \frac{1}{2} \left(\varkappa - \frac{1}{3} \right) r_{xxx} + \frac{1}{360} (19 - 30\varkappa - 45\varkappa^2) r_{xxxxx} + \frac{3}{2} rr_x = o(\mu^9)$$

that is the Kawahara equation (1.4).

4.5. The Whitham scaling regime. If we now assume $\alpha = O(\mu^N)$ for any positive integer N and $s = o(\alpha)$ as $\mu \rightarrow 0$, then we arrive to an example when the Whitham operator W cannot be approximated using a simple differential operator instead. The simplest equation in this case is the Whitham equation

$$r_t + Wr_x + \frac{3}{2}rr_x = o(\mu\alpha^2).$$

An example of the function $\alpha(\mu)$ when the Whitham equation works better than its approximations was given in [26]. At the same time that function $\alpha(\mu)$ may be similar to the Boussinesq scale at some wave-numbers μ as was pointed out in [26].

5. NUMERICAL RESULTS

The purpose of this section is to compare the performance of the Whitham equation as a model for surface water waves to both the KdV equation (1.3) and to the Kawahara equation (1.4). In other words, all these approximate models are compared to the Euler system which is considered as giving the closest description of an actual surface wave profile. For this purpose initial data are imposed, the Whitham, KdV and Kawahara equations are solved with periodic boundary conditions, and the solutions are compared to the numerical solutions of the full Euler equations with free-surface boundary conditions. This matching is made in various scaling regimes from small Stokes numbers to $\mathcal{S} \sim 1$, to large Stokes numbers.

The numerical treatment of the three model equations is a standard spectral scheme, such as used in [16] and [15] for example. For the time stepping, an efficient fourth-order implicit method developed in [12] is used. The numerical treatment of the free-surface problem for the Euler equations is based on a conformal mapping of the fluid domain into a rectangle. In the case of transient dynamics, this method has roots in the work of Ovsyannikov [28], and was later used in [11] and [23]. In the case of periodic boundary conditions, a Fourier-spectral collocation method can be used for the computations, and the particular method used for the numerical experiments reported here is detailed in [25].

Initial conditions for the Euler equations are chosen in such a way that the solutions are expected to be right moving. This can be achieved by imposing an initial surface

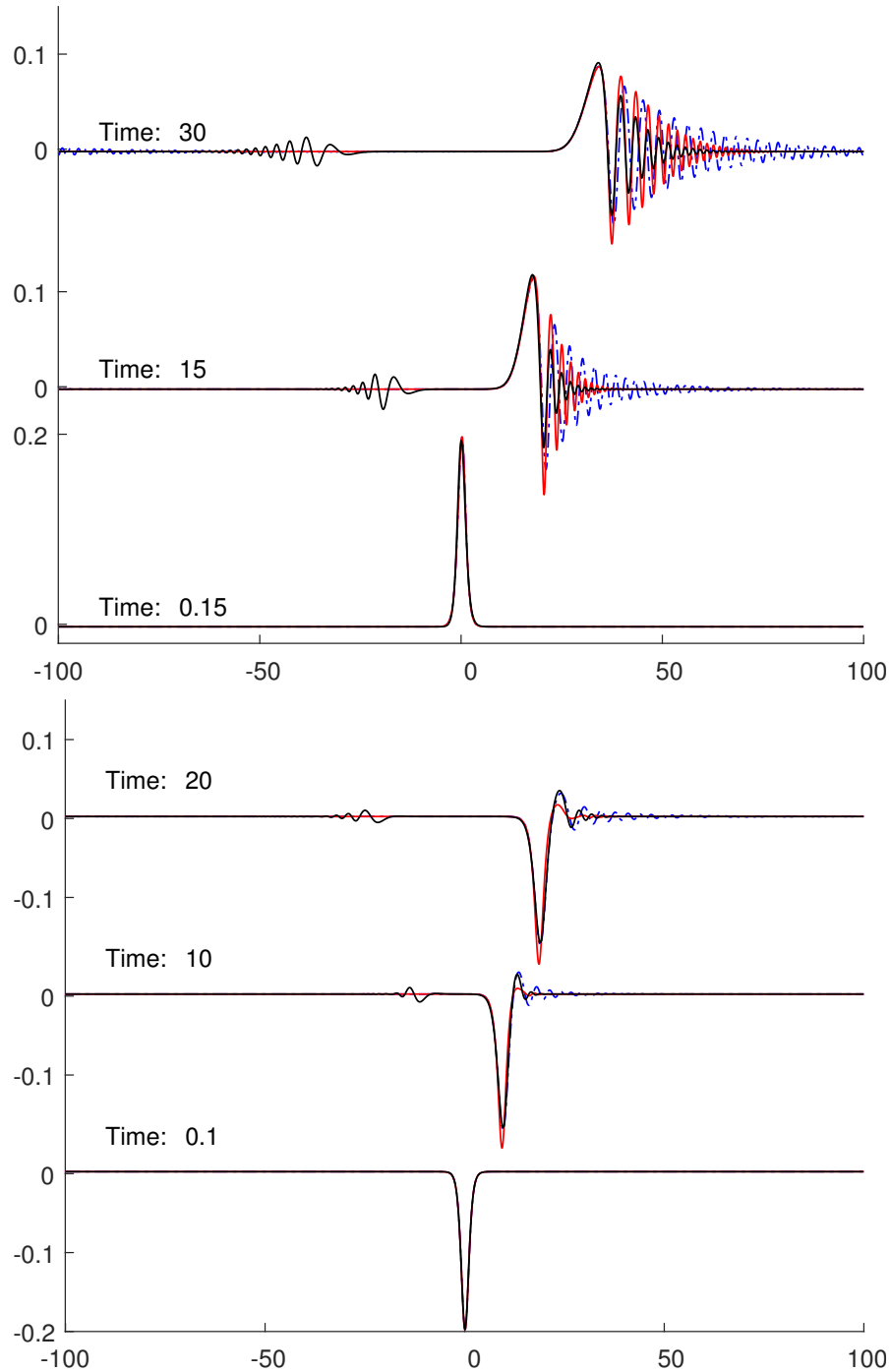


FIGURE 1. Wave profiles at three different times: – the Euler (black line), – Whitham (red line) and – KdV (blue line) with amplitude $\alpha = 0.2$, wavelength $\lambda = \sqrt{5}$ and capillarity parameter $\varkappa = 1/2$.

disturbance η_0 together with the initial trace of the potential $\Phi(x) = \int_0^x \eta_0(\xi) d\xi$. Indeed, the right-going wave condition is $s(x, t) = 0$ which together with (4.3) and (4.5) imply

$$\Phi(x) = \int_0^x u(\xi, 0) d\xi = \int_0^x K^{-1} \eta_0(\xi) d\xi \approx \int_0^x \eta_0(\xi) d\xi.$$

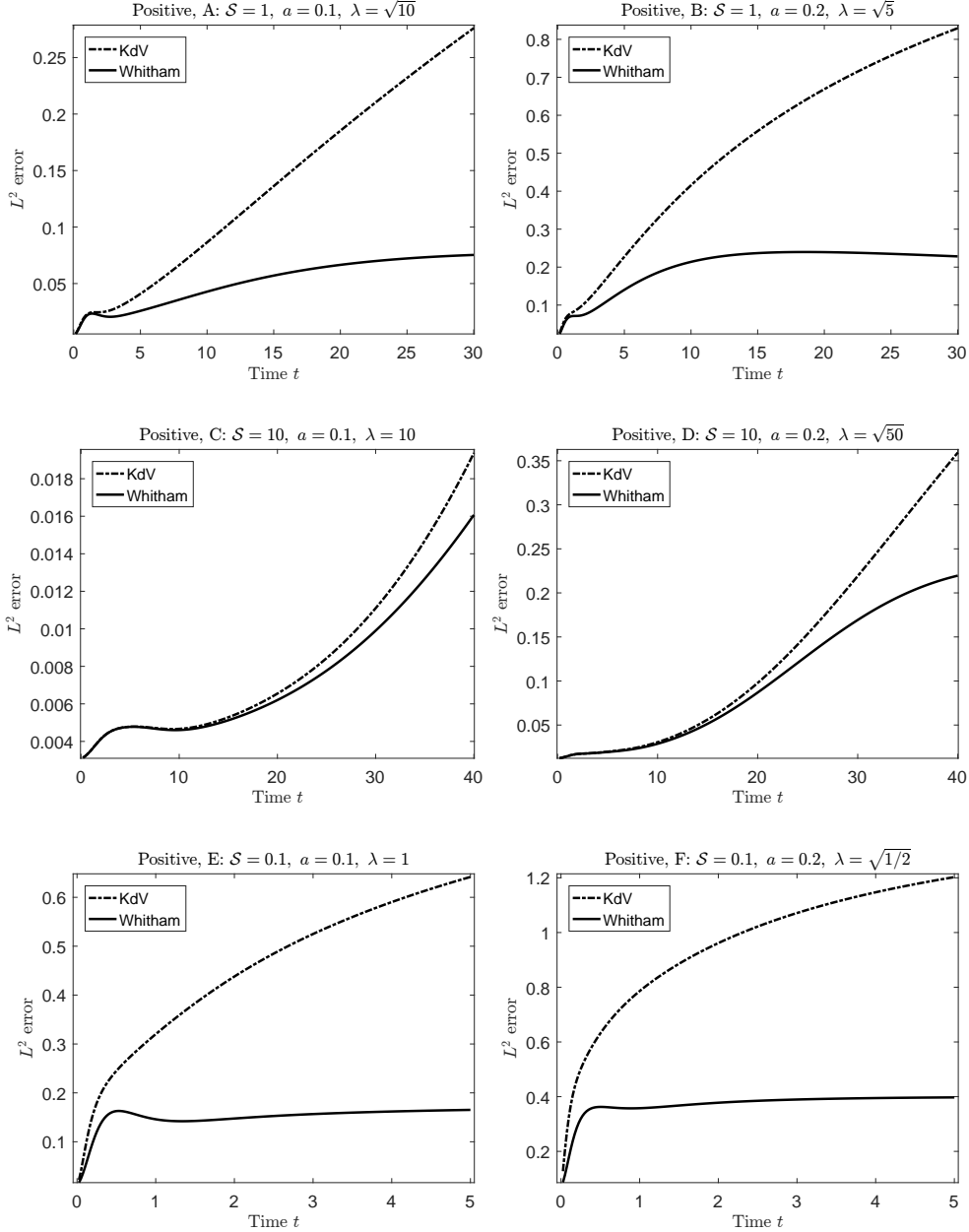


FIGURE 2. L^2 errors in approximation of solutions to the full Euler equations by different model equations with the positive initial wave $\eta_0(x)$ and the surface tension $\varkappa = \frac{1}{2}$.

This last provision makes our numerical experiments more natural, since it is not assumed that the regarded surface waves are strictly right-moving $s = O(\mu^2\alpha)$ and $\eta = r + O(\mu^2\alpha)$. In Figure 1 one can see the corresponding small wave s moving to the left given by solving the Euler system. In order to normalize the data, we choose η_0 in such a way that the average of η_0 over the computational domain is zero. The experiments are performed with several different amplitudes α and wavelengths λ . For the purpose of this section, we define the wavelength λ as the distance between the two points x_1 and x_2 at which

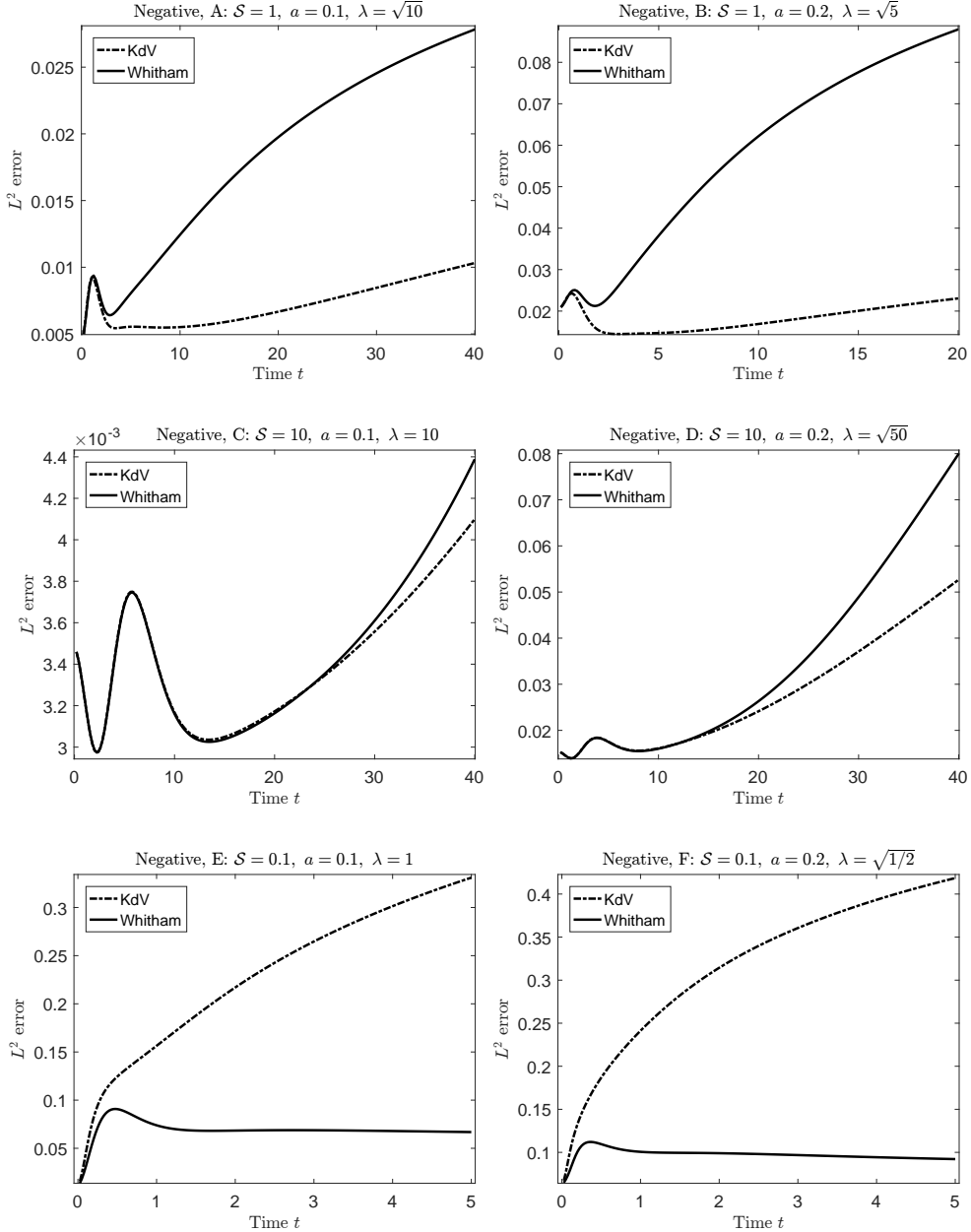


FIGURE 3. L^2 errors in approximation of solutions to the full Euler equations by different model equations with the negative initial wave $\eta_0(x)$ and the surface tension $\varkappa = \frac{1}{2}$.

$\eta_0(x_1) = \eta_0(x_2) = \alpha/2$. Both positive and negative initial disturbances are considered. Numerical experiments were performed with a range of parameters for amplitude α and the wave-length λ . The summary of experiments' settings is given in Table 1. All experiments are made with initial wave of elevation and wave of depression, labeled as “positive” and “negative” respectively. The domain for computations is $-L \leq x \leq L$, with $L = 100$. The “positive” initial data is

$$\eta_0(x) = a \cdot \operatorname{sech}^2(f(\lambda)x) - C, \quad (5.1)$$

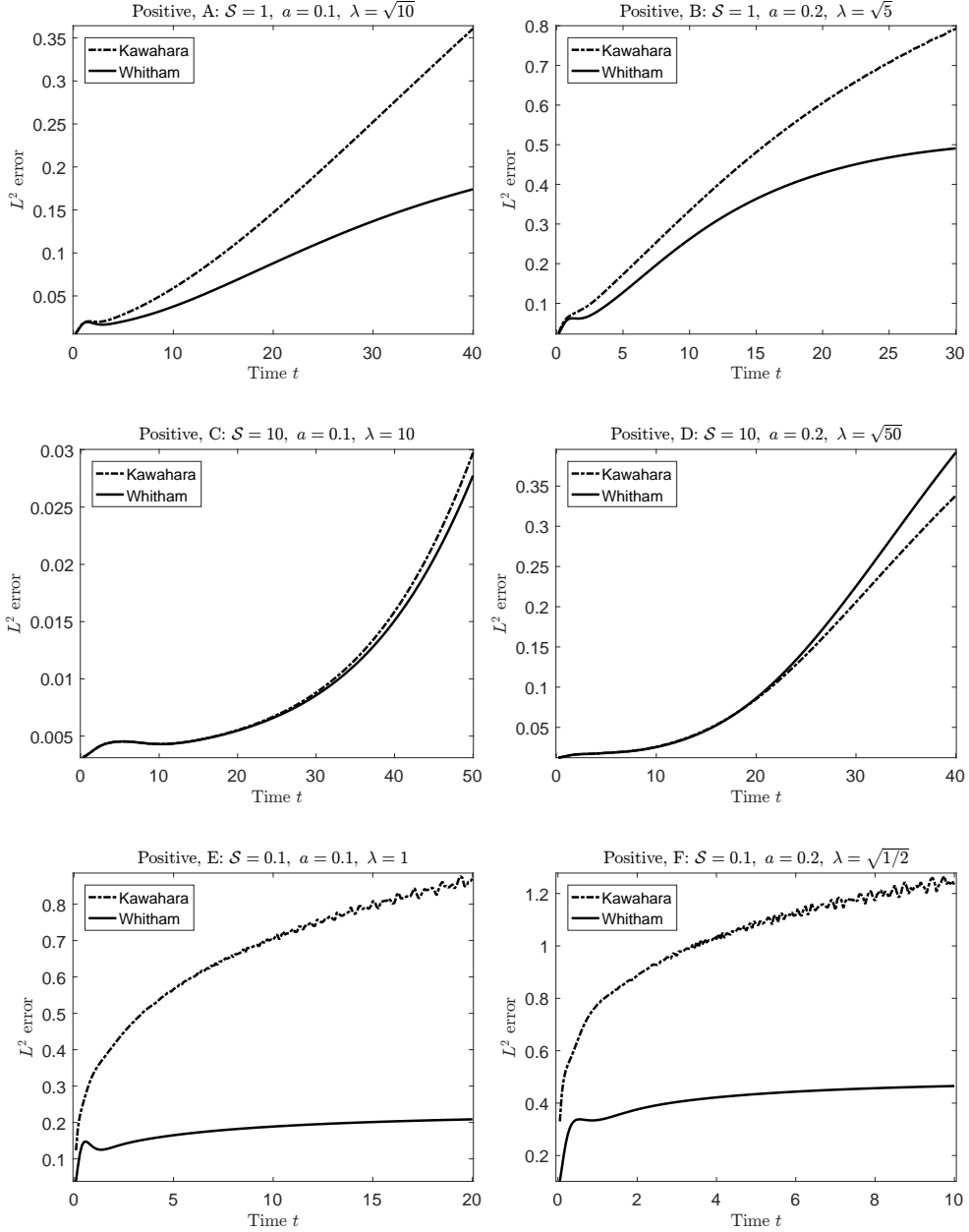


FIGURE 4. L^2 errors in approximation of solutions to the full Euler equations by different model equations with the positive initial wave $\eta_0(x)$ and the surface tension $\varkappa = \frac{1}{3}$.

where

$$f(\lambda) = \frac{2}{\lambda} \log \left(\frac{1 + \sqrt{1/2}}{\sqrt{1/2}} \right), \quad C = \frac{1}{L} \frac{a}{f(\lambda)} \tanh \left(\frac{L}{f(\lambda)} \right).$$

Here C and $f(\lambda)$ are chosen so that $\int_{-L}^L \eta_0(x) dx = 0$, and the wave-length λ is the distance between the two points x_1 and x_2 at which $\eta_0(x_1) = \eta_0(x_2) = a/2$. The velocity potential

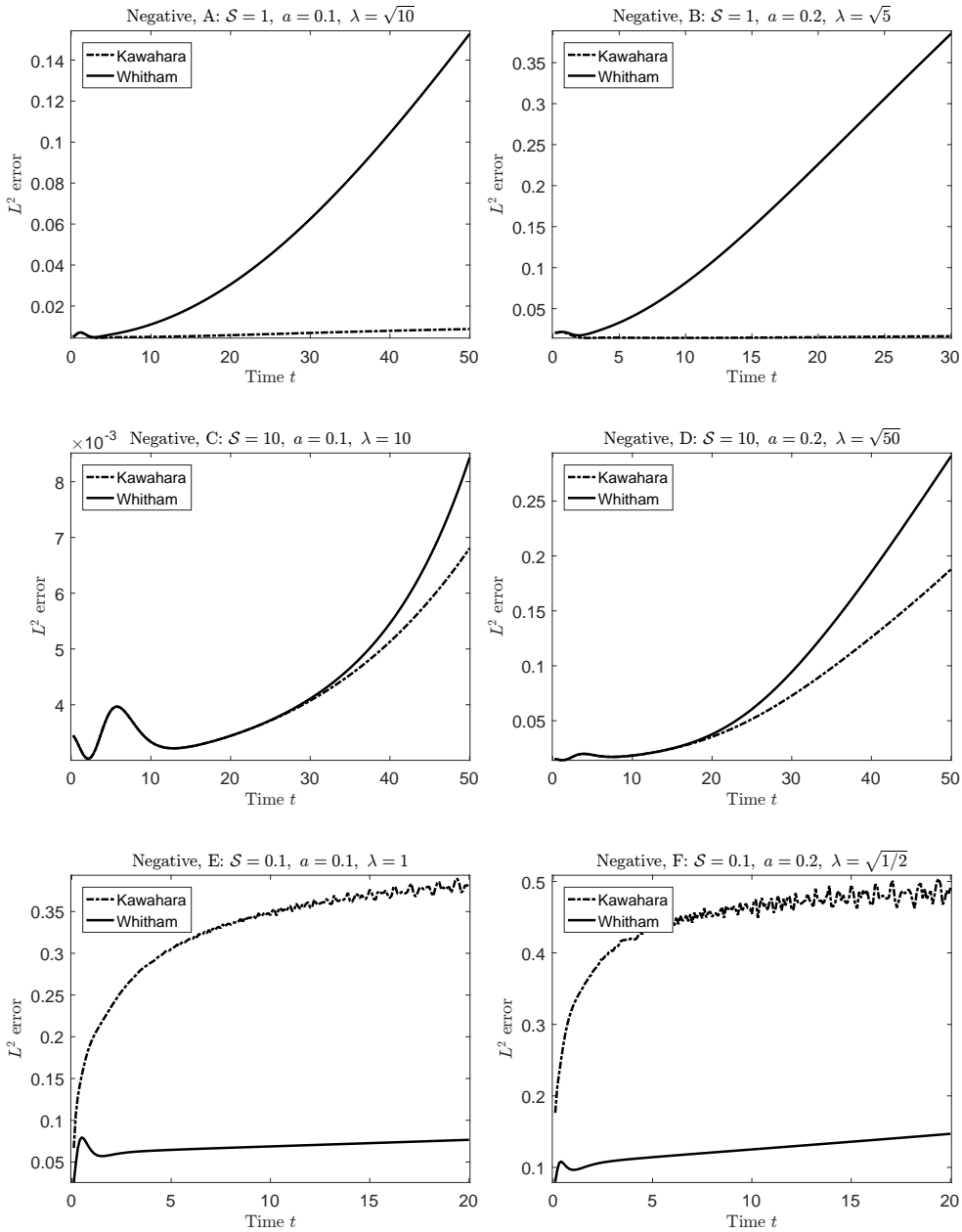


FIGURE 5. L^2 errors in approximation of solutions to the full Euler equations by different model equations with the negative initial wave $\eta_0(x)$ and the surface tension $\varkappa = \frac{1}{3}$.

in this case is:

$$\Phi(x) = \frac{a}{f(\lambda)} \tanh(f(\lambda)x) - Cx, \quad (5.2)$$

The “negative” case function is just the “reverse” of the first one

$$\eta_0(x) = -a \cdot \operatorname{sech}^2(f(\lambda)x) + C. \quad (5.3)$$

The definitions for $f(\lambda)$ and C are the same. And the velocity potential is

$$\Phi(x) = -\frac{a}{f(\lambda)} \tanh(f(\lambda)x) + Cx, \quad (5.4)$$

We calculate solutions of the Whitham equation and the Euler system. We also calculate solutions of the KdV for the capillarity $\varkappa = 1/2$, and solutions of the Kawahara in the case $\varkappa = 1/3$.

In Figure 1, the time evolution of a wave with an initial narrow peak is shown according to the Euler (black line), Whitham (red line) and KdV (blue line) equations. Here the amplitude $\alpha = 0.2$, the wavelength $\lambda = \sqrt{5}$ and the capillary parameter $\varkappa = 1/2$ are used. This case corresponds the Stokes number $S = 1$. It appears that the KdV equation produces a significant amount of spurious oscillations and the Whitham equation gives the closest approximation of the corresponding Euler solution. As one can expect the unidirectional models also lag in the description of waves going to the left.

In order to compare the accuracy of each approximate model we calculate the differences, firstly between the Whitham and Euler equations, and secondly between the KdV (or Kawahara) and Euler equations. These differences are measured in the integral L^2 -norm normalized by initial condition $\|\eta_0\|$ as follows

$$\frac{\|\eta_E(t) - \eta(t)\|}{\|\eta_0\|} = \sqrt{\frac{\int (\eta_E(x, t) - \eta(x, t))^2 dx}{\int \eta_0(x)^2 dx}}$$

where $\eta_E(x, t)$ is the solution for the Euler system and $\eta(x, t)$ corresponds either to the Whitham, KdV or Kawahara equation. The next figures 2, 3, 4, 5 show the dependence of L^2 -error on time for different initial situations. Thus as one can see, the Whitham model performs better than the KdV and Kawahara equations, in nearly all situations except the cases with a negative initial wave of depression and Stokes number approximately unity.

Acknowledgments. This research was supported in part by the Research Council of Norway under grant no. 213474/F20.

REFERENCES

- [1] Aceves-Sánchez, P., Minzoni, A.A. and Panayotaros, P. *Numerical study of a nonlocal model for water-waves with variable depth*, Wave Motion **50** (2013), 80–93.
- [2] T. Alazard, N. Burq and C. Zuily, *On the water-wave equations with surface tension*, Duke Math. Journal **158** (2011), 413–99.
- [3] Biswas A. *Solitary wave solution for the generalized Kawahara equation*, Appl. Math. Lett. **22** (2009), 208–210.
- [4] Benjamin, T. B., Bona, J. L. and Mahony, J. J. *Model equations for long waves in nonlinear dispersive systems*. Philos. Trans. R. Soc. Lond., Ser. A **272** (1972), 47–78.
- [5] Borluk, H., Kalisch, H. and Nicholls, D.P. *A numerical study of the Whitham equation as a model for steady surface water waves*, J. Comput. Appl. Math. **296** (2016) 293–302.
- [6] Chardard, F. *Stabilité des ondes solitaires*, PhD thesis, 2009.
- [7] Choi, W. and Camassa, R. *Exact Evolution Equations for Surface Waves*. J. Eng. Mech. **125** (1999), 756–760.
- [8] Craig, W. and Groves, M.D. *Hamiltonian long-wave approximations to the water-wave problem*. Wave Motion **19** (1994), 367–389.
- [9] Craig, W., Guyenne, P. and Kalisch, H. *Hamiltonian long-wave expansions for free surfaces and interfaces*. Comm. Pure Appl. Math. **58** (2005), 1587–1641.
- [10] Craig, W. and Sulem, C. *Numerical simulation of gravity waves*. J. Comp. Phys. **108** (1993), 73–83.

- [11] Dyachenko, A.I., Kuznetsov, E.A., Spector, M.D. and Zakharov, V.E. *Analytical description of the free surface dynamics of an ideal fluid (canonical formalism and conformal mapping)*. Phys. Lett. A **221** (1996), 73–79.
- [12] De Frutos, J. and Sanz-Serna, J.M. *An easily implementable fourth-order method for the time integration of wave problems*. J. Comp. Phys. **103** (1992), 160–168.
- [13] Ehrnström, M., Groves, M.D. and Wahlén, E. *Solitary waves of the Whitham equation - a variational approach to a class of nonlocal evolution equations and existence of solitary waves of the Whitham equation*. Nonlinearity **25** (2012), 2903–2936.
- [14] Ehrnström, M. and Kalisch, H. *Traveling waves for the Whitham equation*. Differential Integral Equations **22** (2009), 1193–1210.
- [15] Ehrnström, M. and Kalisch, H. *Global bifurcation for the Whitham equation*. Math. Mod. Nat. Phenomena **8** (2013), 13–30.
- [16] Fornberg, B. and Whitham, G.B. *A Numerical and Theoretical Study of Certain Nonlinear Wave Phenomena*. Phil. Trans. Roy. Soc. A **289** (1978), 373–404.
- [17] Hammack, J.L. and Segur, H. *The Korteweg-de Vries equation and water waves. Part 2. Comparison with experiments*. J. Fluid Mech. **65** (1974), 289–314.
- [18] Hur, V.M. and Johnson, M. *Modulational instability in the Whitham equation of water waves*. Studies in Applied Mathematics **134** (2015), 120–143.
- [19] Hur, V.M. and Johnson, M. *Modulational instability in the Whitham equation with surface tension and vorticity*. Nonlinear Anal. **129** (2015), 104–118.
- [20] Kawahara, T. *Oscillatory solitary waves in dispersive media*. J. Phys. Soc. Japan **33** (1972), 260–264.
- [21] Koop, C.G. and Butler, G. *An investigation of internal solitary waves in a two-fluid system*. J. Fluid Mech., **112** (1981), 225–251.
- [22] Lannes, D. *The Water Waves Problem*. Mathematical Surveys and Monographs, vol. **188** (Amer. Math. Soc., Providence, 2013).
- [23] Li, Y.A., Hyman, J.M. and Choi, W. *A Numerical Study of the Exact Evolution Equations for Surface Waves in Water of Finite Depth*. Stud. Appl. Math. **113** (2004), 303–324.
- [24] Milewski, P., Vanden-Broeck, J.-M. and Wang, Z. *Dynamics of steep two-dimensional gravity-capillary solitary waves*. J. Fluid Mech. **664** (2010), 466–477.
- [25] Mitsotakis, D., Dutykh, D. and Carter, J.D. *On the nonlinear dynamics of the traveling-wave solutions of the Serre equations*. Wave Motion, to appear.
- [26] Moldabayev, D., Kalisch, H. and Dutykh, D. *The Whitham Equation as a model for surface water waves*, Phys. D **309** (2015), 99–107.
- [27] Nicholls, D.P. and Reitich, F. *A new approach to analyticity of Dirichlet-Neumann operators*. Proc. Roy. Soc. Edinburgh Sect. A **131** (2001), 1411–1433.
- [28] Ovsyannikov, L.V. *To the shallow water theory foundation*. Arch. Mech. **26** (1974), 407–422.
- [29] Peregrine, D.H. *Calculations of the development of an undular bore*. J. Fluid Mech. **25** (1966), 321–330.
- [30] Petrov, A.A. *Variational statement of the problem of liquid motion in a container of finite dimensions*. Prikl. Math. Mekh. **28** (1964), 917–922.
- [31] Sanford, N., Kodama, K., Carter, J. D. and Kalisch, H. *Stability of traveling wave solutions to the Whitham equation*. Phys Lett. A **378** (2014), 2100–2107.
- [32] Whitham, G. B. *Variational methods and applications to water waves*. Proc. Roy. Soc. London A **299** (1967), 6–25.
- [33] Whitham, G. B. *Linear and Nonlinear Waves* (Wiley, New York, 1974).
- [34] Zakharov, V. E. *Stability of periodic waves of finite amplitude on the surface of a deep fluid*. J. Appl. Mech. Tech. Phys. **9** (1968), 190–194.

Paper D

3.3 Paper title

List of authors

Physical Review B, **76**, 035303 (2007)

Explicit Solutions for a Long-Wave Model with Constant Vorticity

Benjamin Segal*, Daulet Moldabayev†, Henrik Kalisch† and Bernard Deconinck*

Abstract

Explicit parametric solutions are found for a nonlinear long-wave model describing steady surface waves propagating on an inviscid fluid of finite depth in the presence of a linear shear current. The exact solutions, along with an explicit parametric form of the pressure and streamfunction give a complete description of the shape of the free surface and the flow in the bulk of the fluid. The explicit solutions are compared to numerical approximations previously given in [1], and to numerical approximations of solutions of the full Euler equations in the same situation [31]. These comparisons show that the long-wave model yields a fairly accurate approximation of the surface profile as given by the Euler equations up to moderate waveheights. The fluid pressure and the flow underneath the surface are also investigated, and it is found that the long-wave model admits critical layer recirculating flow and non-monotone pressure profiles similar to the flow features of the solutions of the full Euler equations.

1 Introduction

Background vorticity can have a significant effect on the properties of waves at the surface of a fluid [19, 24, 26, 30, 32, 35]. In particular, in the seminal paper of Teles da Silva and Peregrine [31], it was found that the combination of strong background vorticity and large amplitude leads to a number of unusual wave shapes, such as narrow and peaked waves and overhanging bulbous waves. In the present contribution, we continue the study of a simplified model equation which admits some of the features found in [31]. The equation, which has its origins in early work of Benjamin [3], has the form

$$\left(Q + \frac{\omega_0}{2}u^2\right)^2 \left(\frac{du}{dx}\right)^2 = -3 \left(\frac{\omega_0^2}{12}u^4 + gu^3 - (2R - \omega_0 Q)u^2 + 2Su - Q^2\right), \quad (1)$$

where we denote the volume flux per unit span by Q , the momentum flux per unit span and unit density corrected for pressure force by S , and the energy density per unit span by R . The gravitational acceleration is g and the constant vorticity is $-\omega_0$. The total flow depth as measured from the free surface to the rigid bottom is given by the function $u(x)$.

Equation (1) was recently studied in [1]. It was found that solutions of this equation exhibit similar properties as solutions of the full Euler equations displayed in [31]. In particular, in [1] an expression for the pressure was developed, and it was shown that the pressure may become non-monotone in the case of strong background vorticity. Indeed, it was shown in [1] that if

*Department of Applied Mathematics, University of Washington, Seattle, WA 98195-2420, USA

†Department of Mathematics, University of Bergen, Postbox 7800, 5020 Bergen, Norway

$|\omega_0|$ is big enough, the maximum fluid pressure at the bed is not located under the wavecrest. Such behavior is usually only found in transient problems (cf. [33]). Moreover in some cases, the pressure near the crest of the wave may be below atmospheric pressure.

The purpose of the present work is two-fold. First, we develop a method by which equation (1) can be solved *exactly*. The resulting solutions are compared to the numerical approximations found in [1] and to some of the solutions of the full Euler equations from [31]. Secondly, more features of the solutions of (1) are discussed. Using a similar analysis as in [1], the streamfunction is constructed, and it is found that solutions of (1) may feature recirculating flow and pressure inversion. These features may have an impact on the study of sediment resuspension. Indeed, while it is generally accepted that the main mechanism for sediment resuspension is turbulence due to flow separation in the presence of strong viscous shear stresses [7, 27, 29], the strongly non-monotone pressure profiles exhibited by the solutions of (1) may represent a more fundamental mechanism for particle suspension than the viscous theory.

The geometric setup of the problem is explained as follows. Consider a background shear flow $U_0 = \omega_0 z$, where ω can be positive or negative (cf. Figure 1). Superimposed on this background flow is wave motion at the surface of the fluid. One may argue that the wave motion itself introduces variations into the shear flow due to the Stokes drift [16, 25]. However for very long waves, the Stokes drift can be compared to the Stokes drift in the KdV equation [5], and it becomes negligible in the long-wave limit. Moreover, as observed by a number of authors [3, 31, 32], a linear shear current can be taken as a first approximation of more realistic shear flows with more complex structures.

If it is assumed that the free surface describes a steady periodic oscillatory pattern, then the flow underneath the free surface can be uniquely determined [10, 23], even in the presence of vorticity. Thus for the purpose of studying periodic traveling waves, one may use a reference frame moving with the wave. This change of reference frame leads to a stationary problem in the fundamental domain of one wavelength. The incompressibility guarantees the existence of the streamfunction ψ and if constant vorticity $\omega = -\omega_0$ is stipulated, the streamfunction satisfies the Poisson equation

$$\Delta\psi = \psi_{xx} + \psi_{zz} = \omega_0, \text{ in } 0 < z < \eta(x) = \psi|_{z=\eta}. \quad (2)$$

As explained in [2, 4], the three parameters Q , S and R are defined as follows. If $\psi = 0$ on the streamline along the flat bottom, then Q denotes the total volume flux per unit width given by

$$Q = \int_0^\eta \psi_z dz. \quad (3)$$

Thus Q is the value of the streamfunction ψ at the free surface. The flow force per unit width S is defined by

$$S = \int_0^\eta \left\{ \frac{P}{\rho} + \psi_z^2 \right\} dz, \quad (4)$$

and the energy per unit mass is given by

$$R = \frac{1}{2}\psi_z^2 + \frac{1}{2}\psi_x^2 + g\eta \text{ on } z = \eta(x). \quad (5)$$

Finally, the pressure can be expressed as

$$P = \rho \left(R - gz - \frac{1}{2}(\psi_x^2 + \psi_z^2) + \omega_0\psi - \omega_0 Q \right), \quad (6)$$

It is well known that the quantities Q and S do not depend on the value of x [4]. Using the fact that S is a constant, the derivation of the model equation (1) can be effected by assuming that the waves are long, scaling z by the undisturbed depth h_0 , x by a typical wavelength L , and expanding in the small parameter $\beta = h_0^2/L^2$. This yields (1) as an approximate model equation describing the shape of the free surface. In order to distinguish from the free surface η in the full Euler description, we call the unknown of equation (1) u which is an approximation of η . The derivation of (1) was given in [1, 4], where it was shown that (1) is expected to be valid as an approximate model equation describing waves on the surface of the shear flow if the wavelength is long compared to the undisturbed depth of the fluid. On the other hand, a detailed analysis of the derivation explained in [1, 4] shows that there are no assumptions on the amplitude of the waves. Thus at least formally, the model (1) can be expected to model waves of intermediate amplitude.

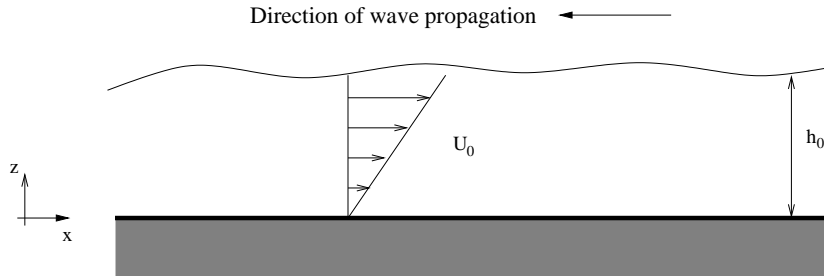


Figure 1: This figure shows the background shear flow $U_0 = \omega_0 z$. In the figure, ω_0 is positive, and the waves which are superposed onto this background current propagate to the left.

2 Explicit solutions

In order to obtain solutions of (1) given in explicit form, we apply the change of variables

$$\frac{dy}{ds} = \frac{du}{dx} \left(Q + \frac{\omega_0}{2} u^2 \right),$$

$$y(s) = u(x).$$

This gives us a new equation for $y(s)$ in the form

$$\left(\frac{dy}{ds} \right)^2 = -3 \left(\frac{\omega_0^2}{12} y^4 + gy^3 - (2R - \omega_0 Q)y^2 + 2Sy - Q^2 \right), \quad (7)$$

and the relation

$$\frac{ds}{dx} = \frac{1}{Q + y^2 \omega_0 / 2}. \quad (8)$$

Integrating (8) we have

$$x(s) = \int^s \left(Q + \frac{\omega_0}{2} y^2 \right) d\xi - x_1. \quad (9)$$

where x_1 is a constant of integration, written explicitly for convenience. We want to solve (7) for $y(s)$ and plug our solution into (9). We notice that in the variables y and $\frac{dy}{ds}$ the equation describes an elliptic curve of genus one [14]. Hermite's Theorem [34, p. 394] states that for a uniform solution to exist we need $\int ds$ to be an abelian integral of the first kind. This condition

is indeed satisfied and we proceed with using a birational transformation to put (7) in the standard Weierstraß form

$$\left(\frac{dy_0}{dx_0}\right)^2 = 4y_0^3 - g_2y_0 - g_3, \quad (10)$$

where the transformation is given as

$$x_0 = -\frac{24(-2\sqrt{12}Q^2y^2\omega_0 - \sqrt{12}Qgy^3 + 4\sqrt{12}QRy^2 + 4\sqrt{12}Q^3 - 6\sqrt{12}QSy + 8Q^2\frac{dy}{ds} - 4\frac{dy}{ds}Sy)}{y^3},$$

$$y_0 = \frac{4(-Qy^2\omega_0 + 2Ry^2 + \frac{dy}{ds}\sqrt{12}Q + 6Q^2 - 6Sy)}{y^2}, \quad (11)$$

and g_2 and g_3 are the lattice invariants

$$g_2 = -768QR\omega_0 + 768R^2 - 1152Sg,$$

$$g_3 = 2048Q^3\omega_0^3 - 6144Q^2R\omega_0^2 - 6912Q^2g^2 + 6144QR^2\omega_0 - 4608QSg\omega_0 + 2034S^2\omega_0^2 - 4096R^3 + 9216RSg.$$

It is well known that the solution to (10) is $y_0(x_0) = \wp(x_0 + c_0; g_2, g_3)$, where \wp is the Weierstraß P function and c_0 is an arbitrary constant [6, 14]. We invert the birational transformation to determine the exact solution to (7) as

$$y(s) = \frac{A + B\wp'((s + c_0)/4; g_2, g_3) + C\wp((s + c_0)/4; g_2, g_3)}{\wp^2((s + c_0)/4; g_2, g_3) + D\wp((s + c_0)/4; g_2, g_3) + E},$$

with

$$A = -288Q^2g - 96Q\omega_0S + 192RS,$$

$$B = \sqrt{12}Q,$$

$$C = -24S,$$

$$D = 8Q\omega_0 - 16R,$$

$$E = 64Q^2\omega_0^2 - 64QR\omega_0 + 64R^2.$$

This gives us $u(x(s))$ in the form

$$u(x(s)) = \frac{A + B\wp'((s + c_0)/4; g_2, g_3) + C\wp((s + c_0)/4; g_2, g_3)}{\wp^2((s + c_0)/4; g_2, g_3) + D\wp((s + c_0)/4; g_2, g_3) + E}, \quad (12)$$

as a function of the parameter s . If we express $x(s)$ as a function of s , then we have a parametric representation for $u(x)$, the surface elevation. From (9) we have

$$x(s) = Qs - x_1 + \frac{\omega_0}{2} \int^s y^2(\xi) d\xi. \quad (13)$$

Expanding and simplifying $y(s)^2$ gives

$$y^2 = \frac{4B\wp^3 + C^2\wp^2 + (2AC - B^2g_2)\wp + (A^2 - B^2g_3)}{(\wp^2 + D\wp + E)^2} + \frac{2AB - 2BC\wp}{(\wp^2 + D\wp + E)^2}\wp', \quad (14)$$

making use of the shorthand $\wp = \wp((s + c_0)/4; g_2, g_3)$ and $\wp' = \wp'((s + c_0)/4; g_2, g_3)$. Plugging (14) into (13) and integrating gives

$$\begin{aligned} x(s) = & Qs - x_1 + \omega_0 B \left[\frac{8(2A - CD) \arctan \left(\frac{D+2\wp}{\sqrt{-D^2+4E}} \right)}{(-D^2 + 4E)^{3/2}} + \frac{-4AD + 8CE + (-8A + 4CD)\wp}{(D^2 - 4E)(\wp^2 + D\wp + E)} \right] \\ & + \frac{\omega_0}{2} \int^s \frac{4B\wp^3 + C^2\wp^2 + (2AC - B^2g_2)\wp + (A^2 - B^2g_3)}{(\wp^2 + D\wp + E)^2} d\xi. \end{aligned} \quad (15)$$

To evaluate the integral in (15) we let

$$m_1 = -\frac{D}{2} - \frac{\sqrt{D^2 - 4E}}{2},$$

$$n_1 = -\frac{D}{2} + \frac{\sqrt{D^2 - 4E}}{2},$$

denote the roots of $\wp^2 + D\wp + E = 0$. The integrand can be split into its components

$$\frac{4B\wp^3 + C^2\wp^2 + (2AC - B^2g_2)\wp + (A^2 - B^2g_3)}{(\wp - m_1)^2(\wp - n_1)^2} = \frac{J(m_1, n_1)}{(\wp - m_1)^2} + \frac{K(m_1, n_1)}{\wp - m_1} + \frac{J(n_1, m_1)}{(\wp - n_1)^2} + \frac{K(n_1, m_1)}{\wp - n_1},$$

with

$$J(m_1, n_1) = \frac{A^2 - B^2g_3 + 2ACm_1 - B^2g_2m_1 + C^2m_1^2 + 4B^2m_1^3}{D^2 - 4E},$$

$$K(m_1, n_1) = \frac{-2A^2 + 2B^2g_3 - 2ACm_1 + B^2g_2m_1 + 4B^2m_1^3 - 2ACn_1 + B^2g_2n_1 - 2C^2m_1n_1 - 12B^2m_1^2n_1}{(4E - D^2)^{3/2}}.$$

Letting

$$\alpha = \wp^{-1}(m_1),$$

$$\beta = \wp^{-1}(n_1),$$

and

$$x_1 = -c_0 Q + x_2,$$

where x_2 is another arbitrary constant, we express $x(s)$ as

$$\begin{aligned} x(s) = & Q(s + c_0) - x_2 + \omega_0 B \left[\frac{8(2A - CD) \arctan \left(\frac{D+2\wp}{\sqrt{-D^2+4E}} \right)}{(-D^2 + 4E)^{3/2}} + \frac{-4AD + 8CE + (-8A + 4CD)\wp}{(D^2 - 4E)(\wp^2 + D\wp + E)} \right] \\ & + 2\omega_0 [J(m_1, n_1)I_2((s + c_0)/4, \alpha) + K(m_1, n_1)I_1((s + c_0)/4, \alpha) \\ & + J(n_1, m_1)I_2((s + c_0)/4, \beta) + K(n_1, m_1)I_1((s + c_0)/4, \beta)], \end{aligned} \quad (16)$$

where I_1 and I_2 come from [6] and [21] and are expressed as

$$I_1(u, \gamma) = \frac{1}{\wp'(\gamma)} \left[\log \left(\frac{\sigma(u - \gamma)}{\sigma(u + \gamma)} \right) + 2u\zeta(\gamma) \right],$$

$$I_2(u, \gamma) = \frac{\wp''(\gamma)}{\wp'^3(\gamma)} \log \left(\frac{\sigma(u + \gamma)}{\sigma(u - \gamma)} \right) - \frac{1}{\wp'^2(\gamma)} (\zeta(u + \gamma) + \zeta(u - \gamma)) - \left(\frac{2\wp(\gamma)}{\wp'^2(\gamma)} + \frac{2\wp''(\gamma)\zeta(\gamma)}{\wp'^3(\gamma)} \right) u.$$

Here ζ is the Weierstraß zeta function and σ is the Weierstraß sigma function. Thus we have $x(s)$ given in (16) and $u(x(s))$ given in (12) both as functions of s . This gives a parametric representation of our solution as a function of s

$$\begin{cases} y = u(x(s)), & \text{given in (12),} \\ x = x(s), & \text{given in (16).} \end{cases} \quad (17)$$

The approximation to the pressure given in [1] is

$$P = \rho \left\{ R - gz - \frac{1}{2} \left(\frac{Q}{u^2} + \frac{\omega_0}{2} \right)^2 (z^2 u'^2 + u^2) + \frac{1}{2} \left(\frac{\omega_0}{6} u^3 - \frac{\omega_0}{2} z^2 u - \frac{2}{3} \omega_0 z^3 - \frac{Q}{3} u + z^2 \frac{Q}{u} \right) \times \left(2Q \frac{u'^2}{u^3} - u'' \left(\frac{Q}{u^2} + \frac{\omega_0}{2} \right) \right) \right\}. \quad (18)$$

This leads to a parametric representation of the pressure as a function of s

$$\begin{cases} y = P(u(x(s)), z), & \text{given in (18),} \\ x = x(s), & \text{given in (16),} \end{cases} \quad (19)$$

where z is the distance from the channel bed.

Finally, note that an expression for the streamfunction can be derived using the techniques of [1]. Since this was not done in [1], the derivation is outlined in the appendix for the sake of completeness. The expression for the streamfunction is

$$\psi = \frac{1}{2} z^2 \omega_0 + z \left(\frac{Q}{u} - \frac{u \omega_0}{2} + \frac{Qu'^2}{3u} - \frac{Qu''}{6} - \frac{\omega_0 u^2 u''}{12} \right) - \frac{z^3}{6} \left(\frac{2Qu'^2}{u^3} - \frac{Qu''}{u^2} - \frac{\omega_0 u''}{2} \right), \quad (20)$$

which gives a parametric representation of the streamfunction as a function of s as

$$\begin{cases} y = \psi(u(x(s)), z), & \text{given in (20),} \\ x = x(s), & \text{given in (16).} \end{cases} \quad (21)$$

3 Matching the explicit solutions to previous works

First, we verify the explicit solutions found here and the numerical approximations given in [1] by comparing them to each other. Following the analysis of [1], we first note that (1) can be written in the form

$$u'^2 = \frac{\mathcal{G}(u)}{\mathcal{F}(u)}. \quad (22)$$

Letting Z_1 , Z_2 , m and M represent the roots of the numerator \mathcal{G} on the right-hand side of (22) we write

$$\begin{aligned} \mathcal{G}(u) &= -3 \left(\frac{\omega_0^2}{12} u^4 + gu^3 - (2R - \omega_0 Q)u^2 + 2Su - Q^2 \right) \\ &= \frac{\omega_0^2}{4} (M - u)(u - m)(u - Z_1)(u - Z_2). \end{aligned} \quad (23)$$

By comparing the coefficients of (23) and assuming that Q , m , and M are given, the two additional roots Z_1 and Z_2 are found as (note that a small typo in [1] has been corrected here)

$$Z_1 = \frac{1}{2} \left\{ - \left(\frac{12}{\omega_0^2} g + (M + m) \right) - \sqrt{\left(\frac{12}{\omega_0^2} g + (M + m) \right)^2 + \frac{48Q^2}{\omega_0^2 m M}} \right\},$$

$$Z_2 = \frac{1}{2} \left\{ - \left(\frac{12}{\omega_0^2} g + (M + m) \right) + \sqrt{\left(\frac{12}{\omega_0^2} g + (M + m) \right)^2 + \frac{48Q^2}{\omega_0^2 m M}} \right\}.$$

The total head R and the flow force S are obtained as

$$R = \frac{\omega_0 Q}{2} - \frac{\omega_0^2}{24} (Z_1 Z_2 + m M + (M + m)(Z_1 + Z_2)),$$

$$S = -\frac{\omega_0^2}{24} ((M + m) Z_1 Z_2 + m M (Z_1 + Z_2)).$$

Following the work in [1] there are two cases depending on the sign of ω_0 . If $\omega_0 > 0$, then u'^2 has no singularities and there is a smooth periodic solution if $Z_2 < m < M$. If $\omega_0 < 0$, then u'^2 has two singularities and the parameter space is more restricted. To find the conditions for smooth solutions to exist, we let $\mathcal{F}(u)$ be expressed as

$$\mathcal{F}(u) = \left(Q + \frac{\omega_0}{2} u^2 \right)^2 = \frac{\omega_0^2}{4} (u - A_+)^2 (u - A_-)^2, \quad (25)$$

which reveals that the derivative is singular when u takes the values $A_+ = \sqrt{\frac{2Q}{-\omega_0}}$ and $A_- = -\sqrt{\frac{2Q}{-\omega_0}}$. In the case $\omega_0 < 0$, smooth solutions exist when $M < A_+$. To better understand this condition, we introduce the non-dimensional Froude number

$$F = \frac{\omega_0 M^2}{2Q}.$$

Substituting F for ω_0 we find four cases:

$$\begin{cases} 0 < F : & \text{smooth solutions exist if } Z_2 < m < M, \\ -1 < F < 0 : & \text{smooth solutions exist,} \\ F = -1 : & \text{limiting case of smooth solutions ceasing to exist,} \\ F < -1.1 : & \text{smooth solutions do not exist but overhanging waves are possible.} \end{cases} \quad (26)$$

Only solutions of the first two cases above are seen in [1]. Below we show one representative example of each of the cases. As in [1], we use the parameters

$$g = 9.81; \rho = 1; m = 1.1; Q = 1.2\sqrt{g}; h_0 = \sqrt[3]{g^{-1}Q^2}; \omega_0 = \frac{2QF}{M^2}. \quad (27)$$

For the following figures, we use the following parameters:

$$\begin{cases} 0 < F : & M = 1.3 \text{ and } F = 1.15, \\ -1 < F < 0 : & M = 1.7 \text{ and } F = -0.3, \\ F = -1 : & M = 1.7 \text{ and } F = -1, \\ F < -1.1 : & M = 1.7 \text{ and } F = -1.1. \end{cases}$$

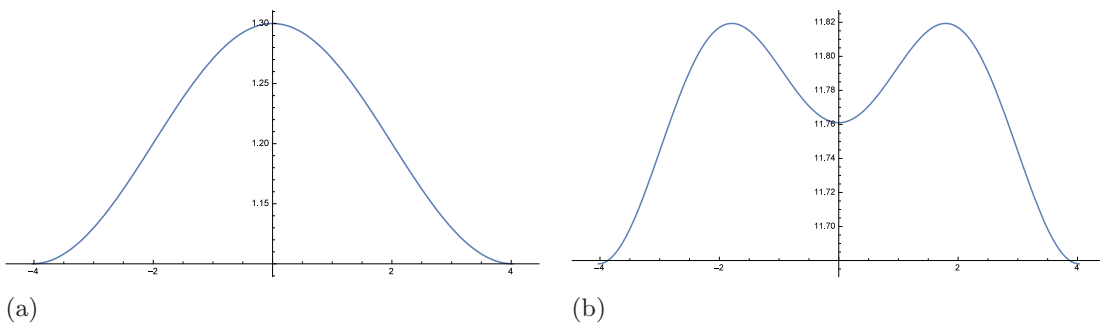


Figure 2: (a) $u(x)$ as a function of x . (b) $P(u(x), 0)$ as a function of x .
 $0 < F, M = 1.3, F = 1.15$, and $-1/2 \leq s \leq 1/2$. Smooth solutions exist.

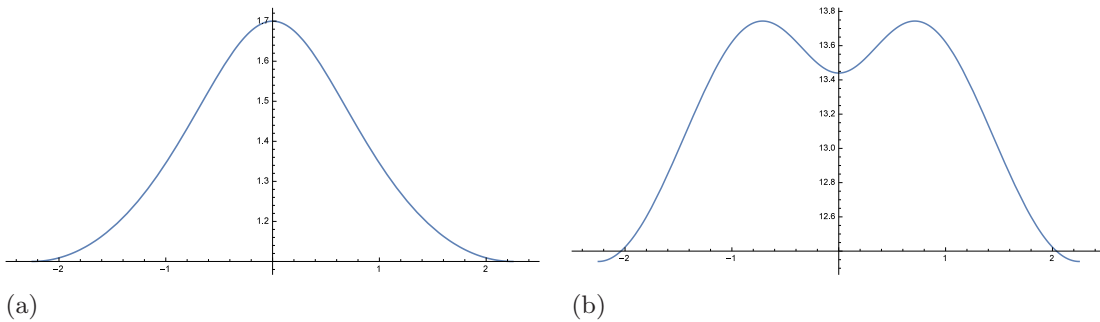


Figure 3: (a) $u(x)$ as a function of x . (b) $P(u(x), 0)$ as a function of x .
 $-1 < F < 0, M = 1.7, F = -0.3$, and $-1/2 \leq s \leq 1/2$. Smooth solutions exist.

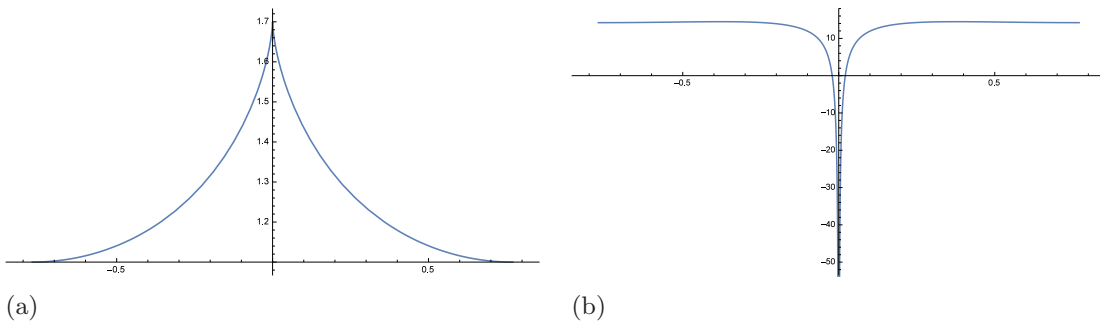


Figure 4: (a) $u(x)$ as a function of x . (b) $P(u(x), 0)$ as a function of x .
 $F = -1, M = 1.7, F = -1$, and $-1/2 \leq s \leq 1/2$. Cusp solution.

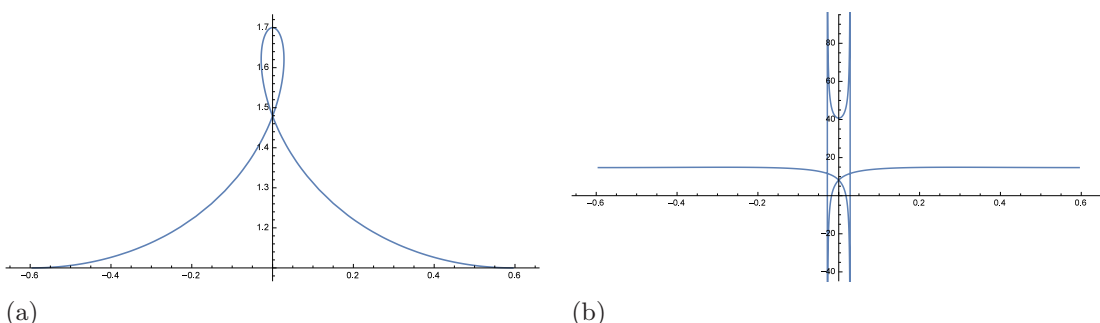


Figure 5: (a) $u(x)$ as a function of x . (b) $P(u(x), 0)$ as a function of x .
 $F < -1, M = 1.7, F = -1.1$, and $-1/2 \leq s \leq 1/2$. Overhanging solutions.

Additionally, in order to obtain periodic solutions with $m < u(x) < M$ and with zero imaginary part, we need to set

$$c_0 = 4\omega_2(g_2, g_3), \quad (28)$$

where ω_2 is a Weierstraß half period corresponding to the lattice invariants g_2 and g_3 with non-zero imaginary part.

We produce plots of the explicit solutions for the various cases of (26) with the parameters given in (27), (28) and (32). Two plots for each case will be shown:

1. $u(x)$ as a function of x ,
2. $P(u(x), 0)$ as a function of x .

Note that since our solutions are symmetric under spacial translations (varying x_2) we can shift the waves so they coincide with those in [1]. Figures 2 and 3 show two curves found in [1], and no visual difference can be detected between the explicit solutions and the numerical approximations of [1]. We notice that $x(s)$ is a monotone function of s as $F > -1$ decreases up until the critical value of $F = -1$. Beyond the critical point where $F = -1$, $x(s)$ is no longer monotone and as a result the solutions are no longer smooth. Figure 4 shows the limiting case of a cusped solution. Note that the evaluation of the pressure at the bottom under the wavecrest appears to yield extremely low and apparently non-physical values. Figure 5 shows a looped (or self-intersecting) solution which is allowed in equations (10) and (11), but not possible in (1). Since it was assumed in the derivation that the free surface is a single-valued function of x , the solution shown in Figure 5 is beyond the physical validity of the equation.

Next we investigate whether the solutions of (1) are close to the solutions of the full Euler equations with a background shear flow found in [31]. Figure 6 and 7 show a sequence of large waveheight solutions with waveheight $H = 1.2$, and for the set of parameters $g = 9.81, \rho = 1.0, h_0 = 1.0$. Note also that by rearranging the variables, we can make the self-intersecting solution look like an overhanging solution. Even though the curves shown in Figure 7 look similar to the free surface profiles shown in Figure 6 of [31], strictly speaking, the curves in Figure 7 do not represent solutions of (1).

We can also set our solutions to be 2π periodic. For this we need to examine the periods of $x(s)$ and $u(s)$. Let ω_1 be the Weierstraß half period corresponding to the lattice invariants g_2 and g_3 with non-zero real part. We note that

$$u(s + T_u) = u(s),$$

where

$$T_u = 8\omega_1,$$

denotes the period of $u(x)$, since both $\wp((s + c_0)/4; g_2, g_3)$ and $\wp'((s + c_0)/4; g_2, g_3)$ are periodic of period $8\omega_1$. Next we notice that

$$x(s + T_u) = x(s) + T_x,$$

where

$$T_x = QT_u + 2\omega_0 [J(m_1, n_1)J_2(\alpha) + K(m_1, n_1)J_1(\alpha) + J(n_1, m_1)J_2(\beta) + K(n_1, m_1)J_1(\beta)],$$

with

$$J_1(\gamma) = \frac{1}{\wp'(\gamma)} (-4\zeta(\omega_1)\gamma + 4\omega_1\zeta(\gamma)),$$

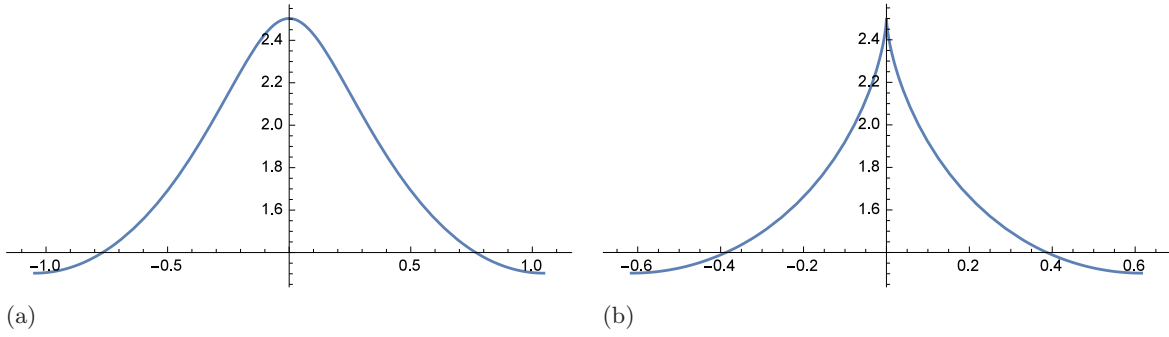


Figure 6: $u(x)$ as a function of x : (a) smooth solution $F = -0.5$, (b) peaked solution $F = -1.0$.

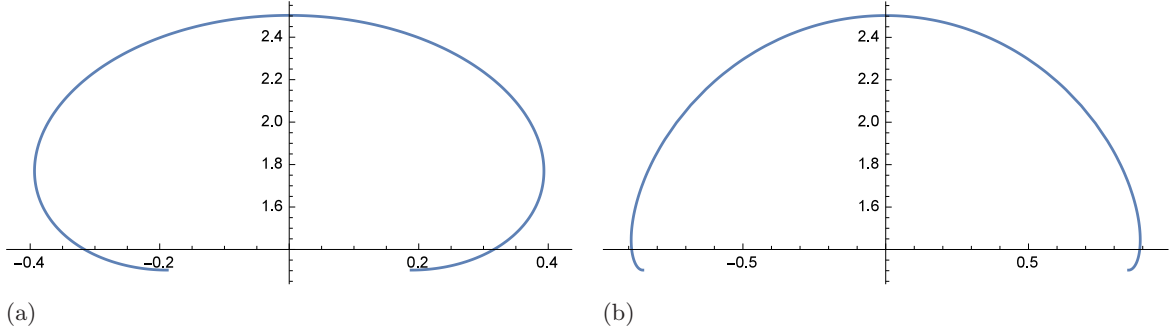


Figure 7: $u(x)$ as a function of x : (a) overhanging solution $F = -2.0$, (b) overhanging solution $F = -3.0$.

and

$$J_2(\gamma) = \frac{\wp''(\gamma)}{\wp^3(\gamma)} 4\zeta(\omega_1)\gamma - \frac{4\zeta(\omega_1)}{\wp'^2(\gamma)} - 2\omega_1 \left(\frac{2\wp(\gamma)}{\wp'^2(\gamma)} + \frac{2\wp''(\gamma)\zeta(\gamma)}{\wp^3(\gamma)} \right).$$

This was determined by noting that

$$I_1(u + 2\omega_1, \gamma) = I_1(u, \gamma) + J_1(\gamma),$$

$$I_2(u + 2\omega_1, \gamma) = I_2(u, \gamma) + J_2(\gamma),$$

which we see from [28]:

$$\zeta(u + 2\omega_1) = \zeta(z) + 2\zeta(\omega_1),$$

$$\sigma(u + 2\omega_1) = -e^{2\zeta(\omega_1)(u+\omega_1)}\sigma(z).$$

Here T_x gives an analytical expression for the wavelength of the solution. If we wanted to force our solutions to be 2π periodic, we could simply rescale x by $2\pi/T_x$ and u by $2\pi/T_x$ as this is the scaling symmetry of (1).

In order to better compare our results with those in [1], we would like to have the peak of the wave at $x = 0$. To achieve this we determine the value of s for which $u(s)$ is at a peak and call this value T_s . Taking (11) we have

$$\wp((T_s + c_0)/4, g_2, g_3) = \frac{4(-QM^2\omega_0 + 2RM^2 + 6Q^2 - 6SM)}{M^2},$$

where we plugged in $y = M$ and $dy/ds = 0$ to be at the peak of the wave. This gives

$$T_s = 4\wp^{-1} \left(\frac{4(-QM^2\omega_0 + 2RM^2 + 6Q^2 - 6SM)}{M^2}, g_2, g_3 \right) - c_0.$$

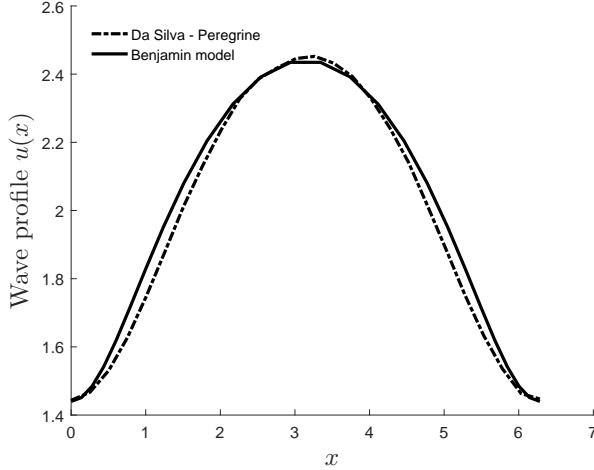


Figure 8: Comparing approximate solutions of the full Euler equations (dashed curve) to exact solutions of (1) (solid curve). The waves have waveheight $H = 1$ and wavelength 2π . The problem is normalized with $g = 1$ and $h_0 = 1$, and the background vorticity is $\omega_0 = -3$.

Thus for solutions with the peak at $x = 0$, we rewrite (17), (19), and (21) as

$$\begin{cases} y = u(T_u(s - T_s)), & \text{given in (12),} \\ x = x(T_u(s - T_s)), & \text{given in (16),} \end{cases} \quad (29)$$

$$\begin{cases} y = P(u(T_u(s - T_s)), z), & \text{given in (18),} \\ x = x(T_u(s - T_s)), & \text{given in (16).} \end{cases} \quad (30)$$

$$\begin{cases} y = \psi(u(T_u(s - T_s)), z), & \text{given in (20),} \\ x = x(T_u(s - T_s)), & \text{given in (16).} \end{cases} \quad (31)$$

Additionally, we set

$$\begin{aligned} x_2 = T_u \left(Q(\tilde{s} + c_0) + \omega_0 B \left[\frac{8(2A - CD) \arctan \left(\frac{D + 2\varphi((\tilde{s} + c_0)/4)}{\sqrt{-D^2 + 4E}} \right)}{(-D^2 + 4E)^{3/2}} \right. \right. \\ \left. \left. + \frac{-4AD + 8CE + (-8A + 4CD)\varphi((\tilde{s} + c_0)/4)}{(D^2 - 4E)(\varphi((\tilde{s} + c_0)/4)^2 + D\varphi((\tilde{s} + c_0)/4) + E)} \right] \right. \\ \left. + 2\omega_0 [J(m_1, n_1)I_2((\tilde{s} + c_0)/4, \alpha) + K(m_1, n_1)I_1((\tilde{s} + c_0)/4, \alpha) \right. \\ \left. + J(n_1, m_1)I_2((\tilde{s} + c_0)/4, \beta) + K(n_1, m_1)I_1((\tilde{s} + c_0)/4, \beta)] \right), \end{aligned} \quad (32)$$

where $\tilde{s} = T_u(0 - T_s)$. This x_2 is chosen so that when $s = 0$, $x = 0$. Additionally, note that we scale s by T_u . The scaling of s is so that as s ranges from $-1/2$ to $1/2$, we plot exactly one period of wavelength T_x .

We compare some wave profiles presented in Fig. 6 of by Teles da Silva and Peregrine [31] with solutions of same parameters computed by the current explicit method. Note that in [31], the parameters g and h_0 were normalized, so that we need to choose $g = 1$ and $h_0 = 1$.

We first present a comparison of a traveling wave of waveheight $H = 1$ and vorticity $\omega_0 = -3$. In order to get a good match with the plot from Fig. 6 of [31], we selected $m = 1.44, M =$

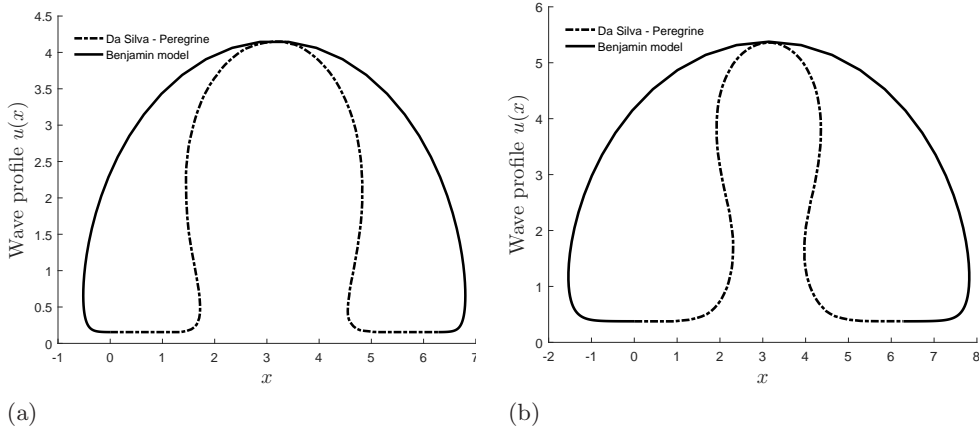


Figure 9: Comparing approximate solutions of the full Euler equations (dashed curve) to exact solutions of (1) (solid curve). The problem is normalized with $g = 1$, $h_0 = 1$ and wavelength 2π . The background vorticity is $\omega_0 = -3$. (a) waveheight $H = 4$. (b) waveheight $H = 5$.

2.44, $Q = 0.09$ Figure 8 shows an explicit solution of (1) compared to a solution of the full Euler equations shown in Fig. 6 in [31]. Even though the waveheight-depth ratio of $1/2$ is not very small, the profiles match fairly closely.

Comparing higher-amplitude waves is more difficult since the solutions shown in [31] with waveheight larger than 1 are overhanging. Setting all parameters correctly yields the comparison shown in Figure 9. As can be seen, the wavelength matches, and the solutions of (7),(8) are also overhanging, but look very different nevertheless. One may conclude from this last comparison, that if solutions of (7),(8) are not single-valued, and therefore are beyond the validity of (1), they will not in general represent the physical reality of the surface-water wave problem.

4 Pressure contours and streamlines

In this section, we explore the flow underneath the surface as predicted by (1), with the help of the expression (18) for the pressure and (20) for the streamfunction.

First, pressure contours and streamlines are reviewed for positive Froude numbers F . This case corresponds to the case labelled 'upstream' in [31]. As mentioned in that work, it is in this case that a critical layer is possible. Examining figures 10-15, it appears that as the strength of the vorticity increases, first, the pressure becomes non-monotone (Figure 11). In other words, the pressure strongly departs from hydrostatic pressure, the bottom pressure is maximal under the sides of the wave (not the crest), and this goes hand in hand with the development of closed streamlines (Figure 12). For large enough Froude numbers, a critical layer (i.e., a closed circulation) develops in the interior of the fluid domain (Figure 13). In the extreme case of $F = 3$, pressure inversion occurs as regions of high pressure are above regions of low pressure in the fluid column (Figure 15).

For negative Froude numbers, the flow corresponds to the downstream case [31]. In this case non-monotone pressures also develop, but no critical layer occurs in the fluid domain. Figures 19 and 20 show strongly non-monotone pressures. Apparently, as the shape of the free surface approaches a cusped profile, non-physical features appear in the description of the flow.

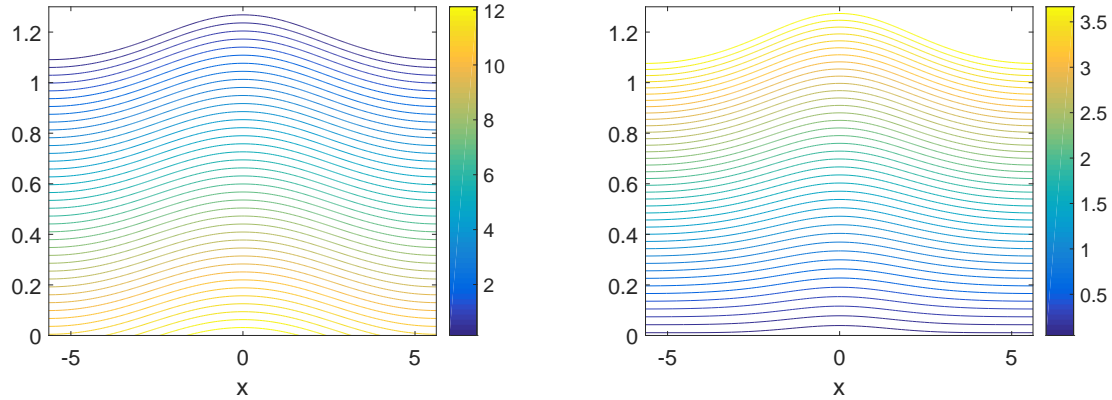


Figure 10: Traveling wave with $m = 1.1$, $M = 1.3$, and $F = 0.2$. Left: pressure contours. Right: streamlines.

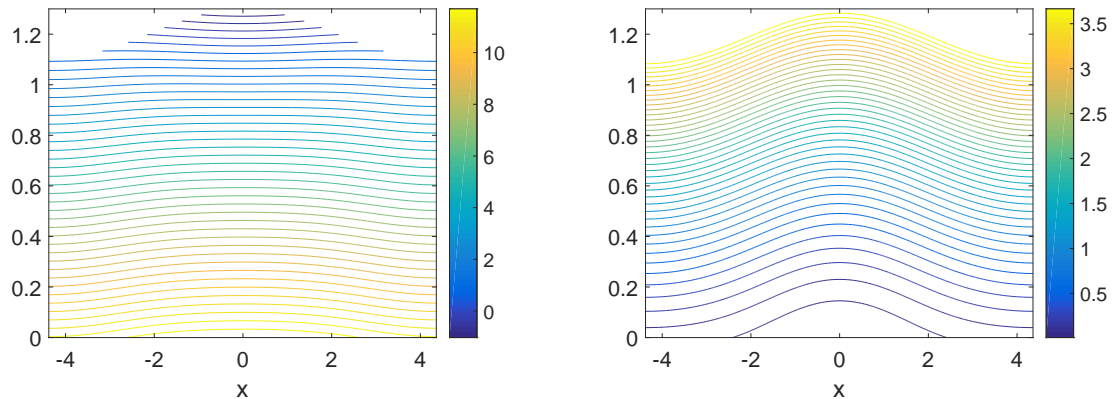


Figure 11: Traveling wave with $m = 1.1$, $M = 1.3$, and $F = 0.9$. Left: pressure contours. Right: streamlines.

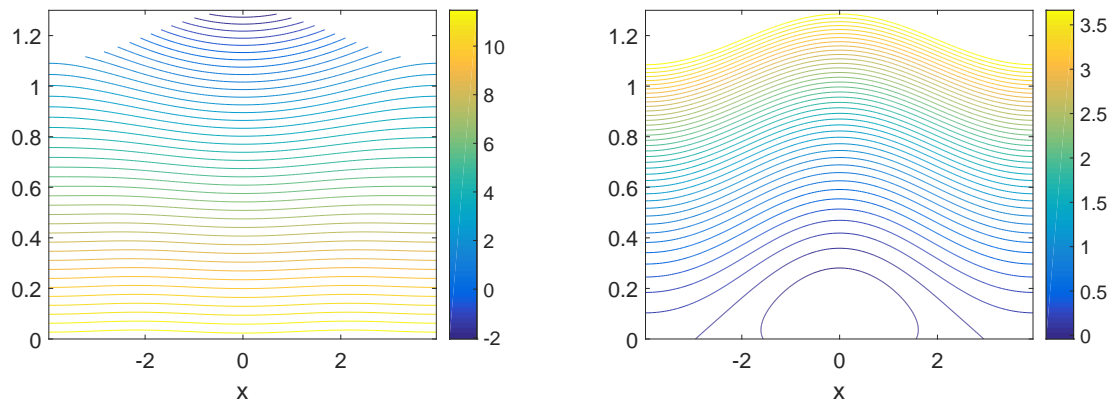


Figure 12: Traveling wave with $m = 1.1$, $M = 1.3$, and $F = 1.2$. Left: pressure contours. Right: streamlines.

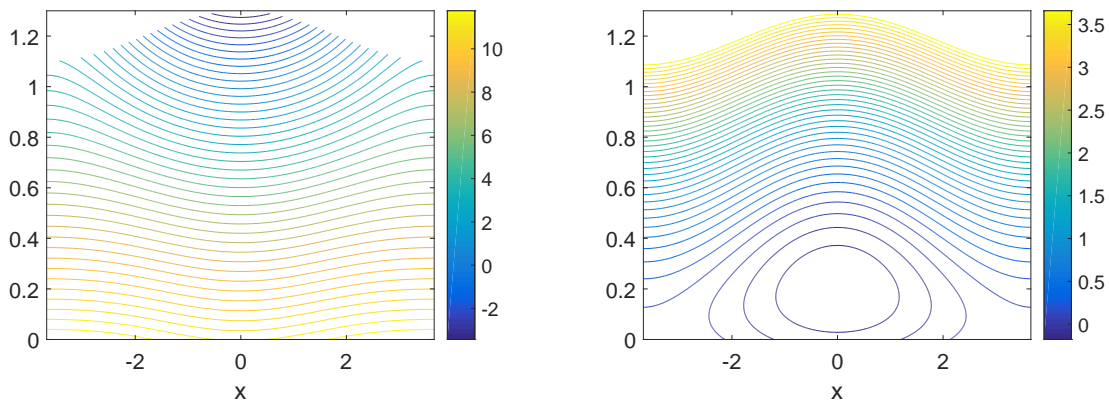


Figure 13: Traveling wave with $m = 1.1$, $M = 1.3$, and $F = 1.5$. Left: pressure contours. Right: streamlines. Pressure highly non-monotone, critical layer appears.

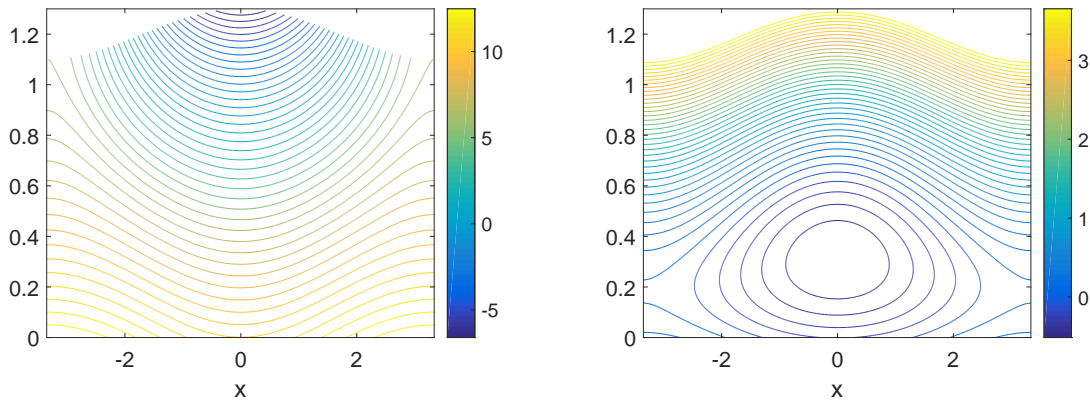


Figure 14: Traveling wave with $m = 1.1$, $M = 1.3$, and $F = 2.0$. Left: pressure contours. Right: streamlines.

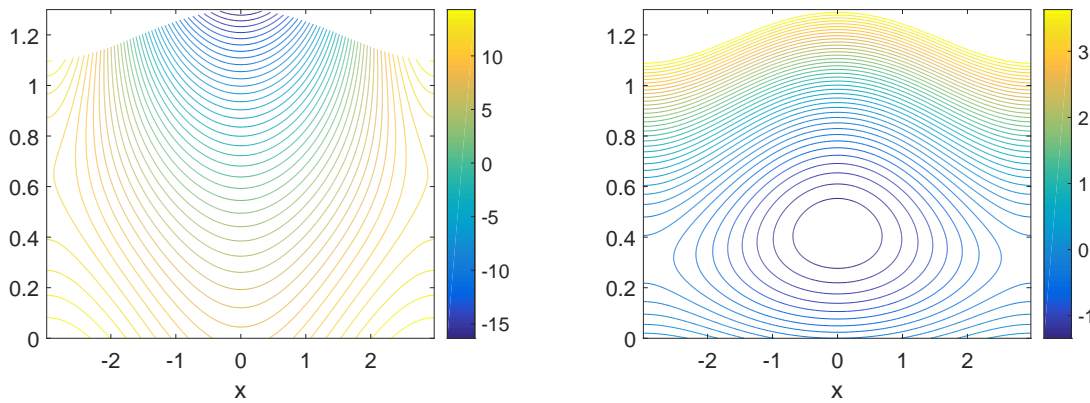


Figure 15: Traveling wave with $m = 1.1$, $M = 1.3$, and $F = 3.0$. Left: pressure contours. Right: streamlines. Pressure inversion: high pressure above low pressure.

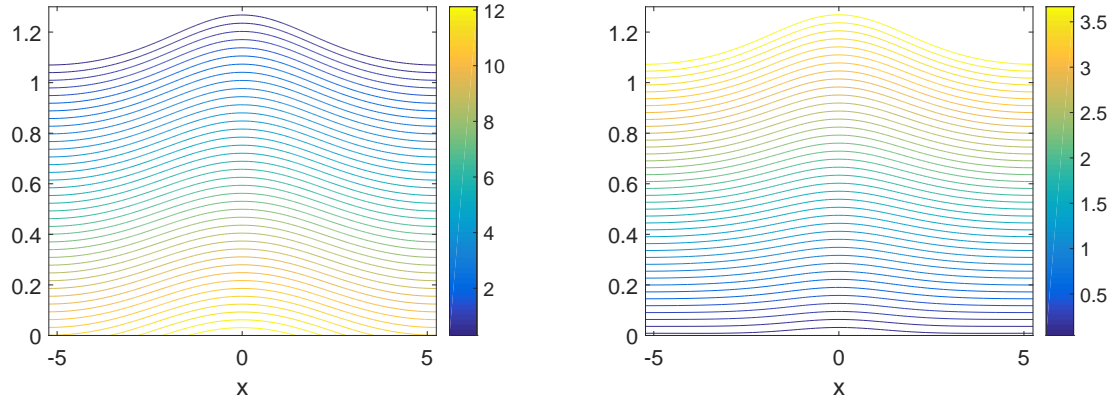


Figure 16: Traveling wave with $m = 1.1$, $M = 1.3$, and $F = -0.001$. Left: pressure contours. Right: streamlines.

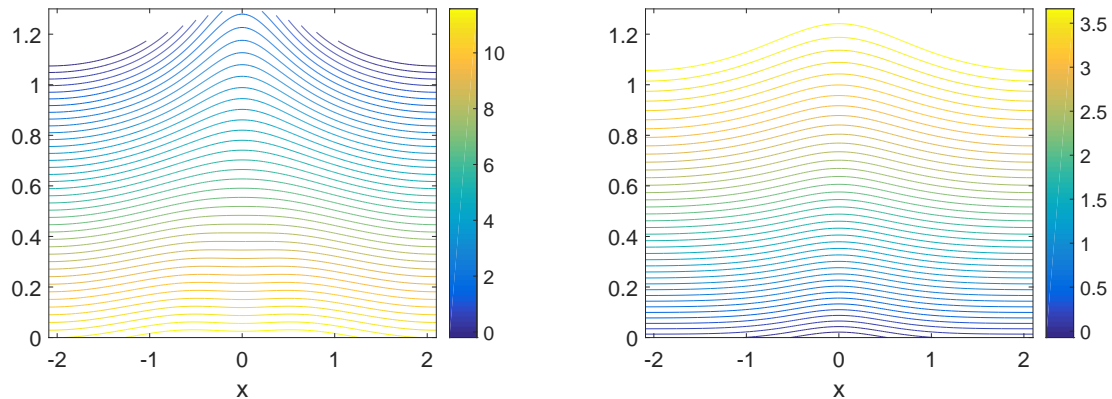


Figure 17: Traveling wave with $m = 1.1$, $M = 1.3$, and $F = -0.5$. Left: pressure contours. Right: streamlines.

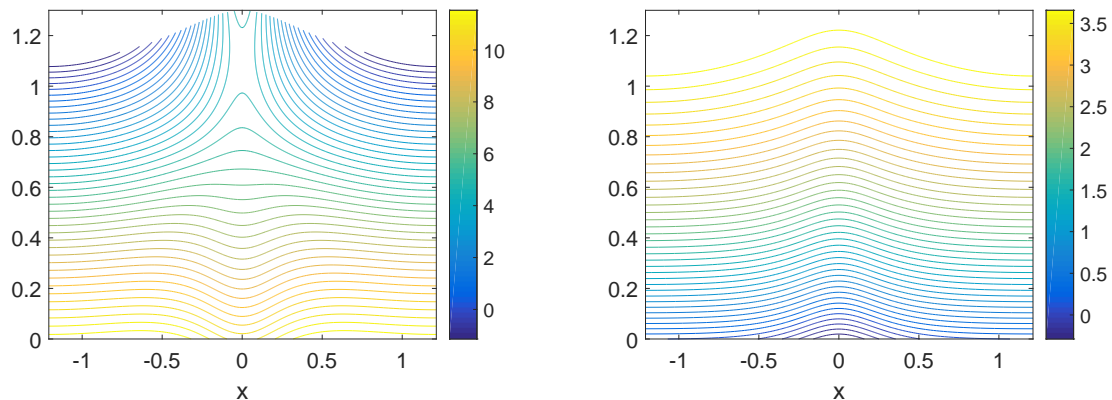


Figure 18: Traveling wave with $m = 1.1$, $M = 1.3$, and $F = -0.7$. Left: pressure contours. Right: streamlines.

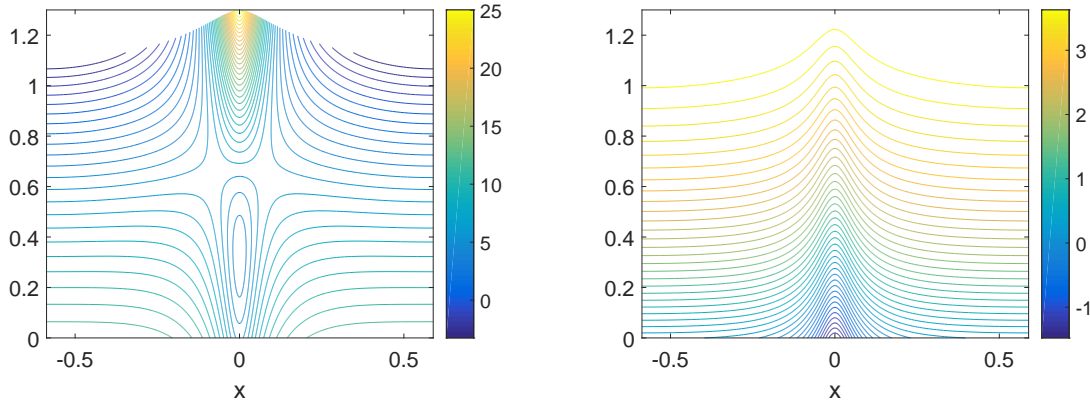


Figure 19: Traveling wave with $m = 1.1$, $M = 1.3$, and $F = -0.9$. Left: pressure contours. Right: streamlines.

5 Conclusion

The nonlinear differential equation (1) is known to be a model for steady surface water waves on a background shear flow. The equation has been found to admit solutions given explicitly in terms of a parametric representation featuring the Weierstraß P, zeta and sigma functions. This representation is a convenient tool for obtaining a variety of wave profiles without having to resort to numerical approximation. In connection with the reconstruction of the pressure underneath the surface explained in [1], and the reconstruction of the streamfunction detailed in the appendix, a complete description of the flow can be obtained.

The exact solutions of (1) have been compared to wave profiles obtained from full Euler computations in [31], and fair agreement was found for regular waves. On the other hand, overhanging waves were found not to agree with the full Euler solutions. This is not surprising since the parametric representation enables the description of multi-valued profiles which transcends the collection of solutions of (1).

With a view towards the flow in the fluid column below the wave, a number of wave shapes with increasing strength of vorticity were exhibited. It was found in the case of steady waves propagating upstream that the flow underneath the waves may feature critical layers and non-monotone pressure profiles. In the case of waves propagating downstream, the development of cusped surface profiles goes hand in hand with unrealistic pressure profiles apparently conflicting with the long-wave approximation which is the basis for the model (1). Building on the results of this paper, future work may focus on detailed comparisons of the fluid flow as described by the methods of the current work to numerical approximations of the flow governed by the Euler equations with background vorticity. Such a study will cast more light on the limitations of the current model, especially as regarding the ability to describe properties of the flow in the bulk of the fluid.

Acknowledgments

This research was supported in part by the Research Council of Norway under grant 213474/F20 and by the National Science Foundation under grant NSF-DMS-1008001. Any opinions, findings, and conclusions

or recommendations expressed in this material are those of the authors and do not necessarily reflect the views of the funding sources.

A Reconstruction of the streamfunction

We want to reconstruct the streamfunction $\psi(x, z)$ using the solutions u of the differential equation (1). This is done by using the ansatz

$$\psi = \frac{1}{2}z^2\omega_0 + zf - \frac{1}{3!}z^3f'', \quad (33)$$

for the streamfunction and the identity

$$Q = \frac{1}{2}u^2\omega_0 + \zeta f - u^3\frac{1}{6}f'',$$

both of which are valid to second order in the long-wave parameter $\beta = h_0^2/\lambda^2$, where h_0 is the undisturbed depth of the fluid, and λ is the wavelength. To obtain an expression for f in terms of ζ , one has to invert the operator $1 - \frac{1}{6}\zeta^2\partial_{xx}$, leading to

$$\left[1 - \frac{1}{6}\zeta^2\partial_{xx}\right]^{-1} \left(\frac{Q}{\zeta} - \frac{1}{2}\zeta\omega_0\right) = f.$$

In order to bring out the difference in scales between the undisturbed depth h_0 and the wavelength L , we use the scaling

$$\tilde{x} = \frac{x}{L}, \quad \tilde{z} = \frac{z}{h_0}, \quad \tilde{\zeta} = \frac{\zeta}{h_0}, \quad \tilde{\psi} = \frac{1}{c_0 h_0} \psi, \quad \tilde{\omega}_0 = \frac{h_0}{c_0} \omega_0,$$

In addition, Q is scaled as

$$\tilde{Q} = \frac{Q}{h_0 c_0}.$$

In non-dimensional variables, the expression for ψ is

$$\tilde{\psi} = \frac{1}{2}\tilde{z}^2\tilde{\omega}_0 + \tilde{z}\tilde{f} - \frac{\beta}{3!}\tilde{z}^3\tilde{f}'' + \mathcal{O}(\beta^2).$$

The function \tilde{f} is written as

$$\begin{aligned} \tilde{f} &= \left[1 + \frac{\beta}{6}\tilde{u}^2\partial_{\tilde{x}}^2 + \mathcal{O}(\beta^2)\right] \left(\frac{\tilde{Q}}{\tilde{u}} - \frac{1}{2}\tilde{u}\omega_0\right) + \mathcal{O}(\beta^2). \\ &= \frac{\tilde{Q}}{\tilde{u}} - \frac{1}{2}\tilde{u}\tilde{\omega}_0 + \frac{\beta}{3}Q\frac{(\tilde{u}')^2}{\tilde{u}} - \frac{\beta}{6}Q\tilde{u}'' - \frac{\beta}{12}\omega_0\tilde{u}^2\tilde{u}'' + \mathcal{O}(\beta^2). \end{aligned}$$

The second derivative is

$$\tilde{f}'' = 2\frac{\tilde{Q}}{\tilde{u}^3}(\tilde{u}')^2 - \frac{\tilde{Q}}{\tilde{u}^2}\tilde{u}'' - \frac{1}{2}\omega_0\tilde{u}'' + \mathcal{O}(\beta).$$

Putting these together, we find the streamfunction in terms of \tilde{u} :

$$\begin{aligned} \tilde{\psi} &= \frac{1}{2}\tilde{z}^2\tilde{\omega}_0 + \tilde{z} \left[\frac{\tilde{Q}}{\tilde{u}} - \frac{1}{2}\tilde{u}\tilde{\omega}_0 + \frac{\beta}{3}Q\frac{(\tilde{u}')^2}{\tilde{u}} - \frac{\beta}{6}Q\tilde{u}'' - \frac{\beta}{12}\omega_0\tilde{u}^2\tilde{u}'' \right] \\ &\quad - \frac{\beta}{3!}\tilde{z}^3 \left[2\frac{Q}{\tilde{u}^3}(\tilde{u}')^2 - \frac{Q}{\tilde{u}^2}\tilde{u}'' - \frac{\omega_0}{2}\tilde{u}'' \right] + \mathcal{O}(\beta^2). \end{aligned}$$

References

- [1] A. Ali and H. Kalisch, *Reconstruction of the pressure in long-wave models with constant vorticity*, Eur. J. Mech. B Fluids **37** (2013), 187–194.
- [2] A. Ali and H. Kalisch, *On the formulation of mass, momentum and energy conservation in the KdV equation*, Acta Appl. Math. **133** (2014), 113–131.
- [3] T. B. Benjamin, *The solitary wave on a stream with an arbitrary distribution of vorticity*, J. Fluid Mech. **12** (1962), 97–116.
- [4] T. B. Benjamin and M. J. Lighthill, *On cnoidal waves and bores*, Proc. Roy. Soc. London Ser. A **224** (1954), 448–460.
- [5] H. Borluk and H. Kalisch, *Particle dynamics in the KdV approximation*, Wave Motion **49** (2012), 691–709.
- [6] P.F. Byrd and M.D. Friedman, Handbook of elliptic integrals for engineers and scientists, vol. 67. (Springer Berlin, 1971).
- [7] T.L. Clarke, B. Lesht, R.A. Young, D.J.P. Swift and G.L. Freeland, *Sediment resuspension by surface-wave action: An examination of possible mechanisms*, Marine Geology, **49** (1982) 43–59
- [8] T. Colin, F. Dias and J.-M. Ghidaglia, *On rotational effects in the modulations of weakly nonlinear water waves over finite depth*, Eur. J. Mech. B Fluids **14** (1995), 775–793.
- [9] A. Constantin, M. Ehrnström and E. Wahlén, *Symmetry of steady periodic gravity water waves with vorticity*, Duke Math. J. **140** (2007), 591–603.
- [10] A. Constantin and J. Escher, *Symmetry of steady periodic surface water waves with vorticity*, J. Fluid Mech. **498** (2004) 171–181.
- [11] A. Constantin and W. Strauss, *Exact steady periodic water waves with vorticity*, Comm. Pure Appl. Math. **57** (2004), 481–527.
- [12] A. Constantin and W. Strauss, *Pressure beneath a Stokes wave*, Comm. Pure Appl. Math. **63** (2010), 533–557.
- [13] A. Constantin and E. Varvaruca, *Steady periodic water waves with constant vorticity: regularity and local bifurcation*, Arch. Ration. Mech. Anal. **199** (2011), 33–67.
- [14] R. Conte and M. Musette, The Painlevé Handbook (Springer Science & Business Media, 2008).
- [15] W. Choi, *Strongly nonlinear long gravity waves in uniform shear flows*, Phys. Rev. E **68** (2003), 026305.
- [16] L. Debnath Nonlinear Water Waves (Academic Press, 1994).
- [17] S.H. Doole, *The pressure head and flowforce parameter space for waves with constant vorticity*, Quart. J. Mech. Appl. Math. **51** (1998), 61–72.
- [18] S.H. Doole and J. Norbury, *The bifurcation of steady gravity water waves in (R, S) parameter space*, J. Fluid Mech. **302** (1995), 287–305.
- [19] M. Ehrnström and G. Villari, *Linear water waves with vorticity: rotational features and particle paths*, J. Differential Equations **244** (2008), 1888–1909,
- [20] M. Ehrnström, J. Escher and E. Wahlén, *Steady water waves with multiple critical layers*, SIAM J. Math. Anal. **43** (2011), 1436–1456.
- [21] I. Gradshteyn and I. Ryzhik, Table of Integrals, Series and Products, 5th edn (Academic Press, New York, 1994).
- [22] V. M. Hur, *Exact solitary water waves with vorticity*, Arch. Ration. Mech. Anal. **188** (2008), 213–244.
- [23] H. Kalisch, *A uniqueness result for periodic traveling waves in water of finite depth*, Nonlinear Anal. **58** (2004), 779–785.
- [24] J. Ko and W. Strauss, *Large-amplitude steady rotational water waves*, Eur. J. Mech. B Fluids **27** (2008), 96–109.
- [25] P.K. Kundu and I.M. Cohen, Fluid Mechanics, 4th edition (Academic Press, 2008)

- [26] Y. Li and S.Å. Ellingsen, *Ship waves on uniform shear current at finite depth: wave resistance and critical velocity*, J. Fluid Mech. **791** (2016), 539–567.
- [27] C.C. Mei, S.-J. Fan and K.-R. Jin, *Resuspension and transport of fine sediments by waves*, J. Geophys. Res. Oceans **102** (1997), 15807–15821.
- [28] F.W.J. Olver, D.W. Lozier, D.F. Boisvert and C.W. Clark, Eds. NIST Handbook of Mathematical Functions, (Cambridge University Press, New York, 2010).
- [29] J.S. Ribberink and A.A. Al-Salem, *Sediment transport in oscillatory boundary layers in cases of rippled beds and sheet flow*, J. Geophys. Res. Oceans **99** (1994), 12707–12727.
- [30] R. Thomas, C. Kharif and M. Manna, *A nonlinear Schrödinger equation for water waves on finite depth with constant vorticity* Phys. Fluids **24** (2012), 127102.
- [31] A.F. Teles da Silva and D.H. Peregrine, *Steep, steady surface waves on water of finite depth with constant vorticity*, J. Fluid Mech. **195** (1988), 281–302.
- [32] J. Touboul, J. Charland, V. Rey and K. Belibassakis, *Extended mild-slope equation for surface waves interacting with a vertically sheared current*, Coastal Engineering **116** (2016), 77–88.
- [33] J. Touboul and E. Pelinovsky, *Bottom pressure distribution under a solitonic wave reflecting on a vertical wall*, Eur. J. Mech. B Fluids **48** (2014), 13–18.
- [34] G. Valiron and J. Glazebrook, The Geometric Theory of Ordinary Differential Equations and Algebraic Functions (Math Sci Press, 1984).
- [35] J.-M. Vanden-Broeck, *Periodic waves with constant vorticity in water of infinite depth*, IMA J. Appl. Math. **56** (1996), 207–217.
- [36] E. Wahlén, *Steady water waves with a critical layer*, J. Differential Equations **246** (2009), 2468–2483.
- [37] E. Wahlén, *Hamiltonian long-wave approximations of water waves with constant vorticity*, Phys. Lett. A **372** (2008), 2597–2602.

Appendix A

Some appendix

Bibliography

- [1] BIRKELAND, T., AND NEPSTAD, R. Pyprop. <http://pyprop.googlecode.com>. 1
- [2] DE BOOR, C. *A Practical Guide to Splines*. Springer-Verlag, New York, 2001. 1